

# 1 **Future volcanic eruptions may delay the recovery of lower** 2 **stratospheric ozone over Antarctica and Southern Hemisphere mid-** 3 **latitudes**

4 Man Mei Chim<sup>1</sup>, Nathan Luke Abraham<sup>2,3</sup>, Thomas J. Aubry<sup>4,5</sup>, Ben Johnson<sup>6</sup>, Hella Garny<sup>7</sup>, Susan  
5 Solomon<sup>8</sup>, and Anja Schmidt<sup>7,9</sup>

6 <sup>1</sup> Department of Mathematics and Statistics, University of Exeter, Exeter, UK

7 <sup>2</sup> National Centre for Atmospheric Science, UK

8 <sup>3</sup> Yusuf Hamied Department of Chemistry, University of Cambridge, Cambridge, UK

9 <sup>4</sup> Department of Earth Sciences, University of Oxford, Oxford, UK

10 <sup>5</sup> Department of Earth and Environmental Sciences, University of Exeter, Penryn, UK

11 <sup>6</sup> Met Office, Exeter, UK

12 <sup>7</sup> German Aerospace Center (DLR), Institute of Atmospheric Physics (IPA), Oberpfaffenhofen, Germany

13 <sup>8</sup> Department of Earth, Atmospheric and Planetary Sciences, Massachusetts Institute of Technology, Cambridge, MA, USA

14 <sup>9</sup> Meteorological Institute, Ludwig-Maximilian University Munich, Munich, Germany

15  
16 *Correspondence to:* Man Mei Chim (m.m.chim@exeter.ac.uk)

17 **Abstract.** Sporadic explosive volcanic eruptions can inject large amounts of sulfur into the stratosphere, which forms volcanic  
18 sulfate aerosols with the potential to affect stratospheric ozone chemistry. Future volcanic eruptions have been represented in  
19 climate projection studies with varying degrees of realism despite their potential importance for polar ozone recovery. Climate  
20 projections typically use a constant volcanic forcing based on a historical average, which very likely underestimates the  
21 magnitude of future volcanic forcing and ignores the sporadic nature of volcanic eruptions. In this study, we use stochastic  
22 volcanic eruption scenarios and a plume-aerosol-chemistry-climate model (UKESM-VPLUME) to assess the effect of future  
23 volcanic sulfur injections on lower stratospheric ozone recovery over Antarctica and Southern Hemisphere mid-latitudes. We  
24 find that sporadic eruptions can delay Antarctic total column ozone recovery by up to five years, though this delay is relatively  
25 small when compared with the long-term ozone recovery timescale. Large-magnitude eruptions occurring before mid-century  
26 can, however, episodically cause more substantial delays in the recovery. Based on a composite analysis we show that the  
27 ozone response to volcanic sulfate aerosols over Antarctica and Southern Hemisphere mid-latitudes weakens over the 21st  
28 century due to declining chlorofluorocarbon concentrations. Overall, our findings underscore the need for fully interactive  
29 volcanic aerosol-chemistry coupling to assess the resilience of the Antarctic ozone layer in response to future volcanic  
30 eruptions and other stratospheric perturbation events. Our results also support previous calls for sustained monitoring of  
31 stratospheric composition and ozone-depleting processes to better anticipate and attribute changes in ozone recovery.

## 32 1 Introduction

33 The stratospheric ozone layer has been slowly recovering since about the year 2000, following the implementation of the  
34 Montreal Protocol in 1987 and its subsequent amendments, which limited the production and consumption of ozone-depleting  
35 substances (ODSs), including chlorofluorocarbons (CFCs) and bromine-containing halons. These ODSs are sufficiently long-  
36 lived to reach the stratosphere where they undergo photolysis, releasing chlorine and bromine atoms that catalytically destroy  
37 ozone. According to WMO/UNEP ozone assessments, polar ozone concentrations are projected to return to their 1980 levels  
38 by 2066 (range: 2049-2077) in Antarctica and by 2045 (range: 2029-2051) in the Arctic (WMO, 2022). Although the Antarctic  
39 ozone layer has shown a robust recovery trend since 2000, as observed and simulated in chemistry-climate models (WMO,  
40 2022), recent years have witnessed large ozone holes related to elevated stratospheric aerosol loading from volcanic eruptions  
41 and wildfires (Solomon et al., 2016; Yu et al., 2021; Solomon et al., 2023). For instance, the 2015 Calbuco eruption in Chile,  
42 with a stratospheric injection of about 0.4 Tg of sulfur dioxide (SO<sub>2</sub>), led to a record-large Antarctic ozone hole exceeding 25  
43 million km<sup>2</sup> in the same year (Solomon et al., 2016; Ivy et al., 2017; Zhu et al., 2018). Model simulations by Stone et al. (2021)  
44 suggest that volcanic sulfate aerosols from the 2015 Calbuco eruption reduced the total column ozone by 1 to 5% over the  
45 entire Southern Hemisphere (SH) mid-latitudes region (up to 32 °S) from August to December. The unpredictability of volcanic  
46 eruptions and other stratospheric perturbation events, such as wildfires, continue to complicate assessments of future ozone  
47 recovery over Antarctica and SH mid-latitudes (Chipperfield and Bekki, 2024).

48  
49 Stratospheric volcanic sulfate aerosols provide surfaces facilitating heterogeneous chemical reactions that catalyse the release  
50 of reactive chlorine and bromine species from their respective reservoir species (Eqn. 1 to 3). At present, volcanic eruptions  
51 that inject sulfur into the stratosphere result in a net decrease in Antarctic column ozone. This is because volcanic sulfate  
52 aerosols enhance ozone loss via the HOx, ClOx, and BrOx catalytic cycles, which dominate over the suppression of ozone loss  
53 driven by the NOx cycle (Eqn. 4). Observational and modelling studies have provided evidence of the reduction in NOx and  
54 enhancement in halogen radicals at mid-latitudes after the 1991 Mt. Pinatubo eruption (Fahey et al., 1993). The ozone response  
55 to volcanic sulfate aerosols is greater over Antarctica than other latitudes due to the extreme cold temperatures and the presence  
56 of polar stratospheric clouds inside the Antarctic polar vortex. As anthropogenic ODSs continue to decline in this century and  
57 assuming no injection of volcanic halogen or unexpected rise in CFC emissions, future volcanic eruptions with the same  
58 stratospheric SO<sub>2</sub> injection are expected to cause less ozone loss via the ClOx and BrOx cycles. Therefore, future enhancements  
59 in stratospheric aerosol loading are anticipated to lead to a net increase in Antarctic column ozone towards the middle or the  
60 end of this century (Klobas et al., 2017).



65  
66  
67 Volcanic eruptions may also inject water vapour and volcanic halogen species into the stratosphere in addition to volcanic SO<sub>2</sub>  
68 and cause additional chemical ozone loss (Bobrowski et al., 2003; Pyle and Mather, 2009; Evan et al., 2023; Santee et al.,  
69 2024). Recent modelling studies demonstrate that the co-injection of volcanic sulfur and halogens into the stratosphere can  
70 lead to greater and prolonged ozone depletion compared to sulfur injections only (Klobas et al., 2017; Brenna et al., 2020;  
71 Ming et al. 2020; Staunton-Sykes et al., 2021). Large amounts of volcanic water vapour injection, as demonstrated by the 2022  
72 Hunga Tonga-Hunga Ha'apai eruption, can also perturb stratospheric ozone for 4-7 years (Zhu et al., 2022; Fleming et al.,  
73 2024; Zhou et al., 2024; Zhuo et al., 2025). While volcanic halogen and water vapor emissions are important for ozone recovery  
74 projections, strong stratospheric water vapor and halogen injections are rare and highly variable. Volcanic SO<sub>2</sub> is the most

Deleted: can break down in the atmosphere

Deleted: the

Deleted: modelled

Deleted: show

Deleted: can

Deleted: pose

Deleted: uncertainties

Deleted: and challenges in assessing

Deleted: the

Moved down [1]: Stratospheric volcanic sulfate aerosols provide a surface facilitating heterogeneous chemical reactions that catalyse the release of reactive chlorine and bromine species from their respective reservoir species (Eqn. 1 to 3).

Moved down [2]: Observational and modelling studies have provided evidence of the reduction in NOx and enhancement in halogen radicals at mid-latitudes after the 1991 Mt. Pinatubo eruption (Fahey et al., 1993).

Moved down [3]:  $\text{ClONO}_2 + \text{H}_2\text{O (aerosol)} \rightarrow \text{HOCl} + \text{HNO}_3$  (Eqn. 1)  
 $\text{BrONO}_2 + \text{H}_2\text{O (aerosol)} \rightarrow \text{HNO}_3 + \text{HOBr}$  (Eqn. 2)

Deleted: ¶

... [1]

Deleted: ¶

... [2]

Deleted: a

Formatted: Not Highlight

Formatted: Not Highlight

Deleted: Fig. 1 illustrates the volcanic effects on Antarctic ozone loss. ... [3]

Deleted: the

Deleted: HOx-, ClOx-, and BrOx-catalysed ozone loss,

Deleted: and

Deleted: the

Formatted: Not Highlight

Formatted: Not Highlight

Formatted: Not Highlight

Deleted: 1 to

Formatted: Not Highlight

Deleted: ¶

Deleted: increases

Formatted: Not Highlight

Moved (insertion) [3]

Formatted: Subscript

Formatted: Pattern: Clear (White)

Formatted: Subscript

141 commonly emitted species with comprehensive ice-core and satellite emission inventories (Carn et al., 2016; Sigl et al., 2021),  
142 whereas volcanic halogen and water vapor injections lack comprehensive records, particularly prior to the satellite era. We  
143 therefore focus only on SO<sub>2</sub> emissions in this study. Apart from volcanic halogen and water vapour emissions, very short-lived  
144 (VSL) chlorine and bromine compounds, which have lifetimes of less than 6 months, are also important sources of stratospheric  
145 bromine and chlorine (Sturges et al., 2000; Dorf et al., 2008; Laube et al., 2008; Sala et al., 2014; Wales et al., 2018), which  
146 can lead to uncertainties in future ozone changes (Klobas et al., 2017; Villamayor et al., 2023).

148 Despite the importance of future volcanic sulfate aerosols enhancements for ozone recovery, few studies have investigated the  
149 effects of future volcanic eruptions on stratospheric ozone over the polar and mid-latitude regions due to the unpredictability  
150 of future eruptions. The first phase of the Chemistry Climate Model Initiative (CCMI-1) included volcanic aerosols in historical  
151 simulations from 1850 to 2014 but assumed zero volcanic forcing in future projections from 2015 to 2100 (Dhomse et al.,  
152 2018; Eyring et al., 2013). In CCMI-2, the model experiments adopted the Coupled Model Intercomparison Project (CMIP6)  
153 protocol, using a prescribed constant volcanic forcing equivalent to the 1850-2014 mean volcanic forcing in future projections  
154 from 2015 to 2100 (O'Neill et al., 2016). Naik et al. (2017) adopted a similar approach, prescribing a constant volcanic forcing  
155 equivalent to the 1860-1999 mean to examine the volcanic effects on stratospheric ozone recovery. They concluded that  
156 stratospheric volcanic sulfate aerosols enhancements in two future RCP scenarios had no impact on the polar ozone return  
157 dates (Naik et al., 2017), but their model did not reproduce the chemical perturbations documented by Fahey et al. (1993)  
158 following 1991 Mt. Pinatubo. Further, the use of a prescribed and constant volcanic forcing does not represent the sporadic  
159 nature of volcanic eruptions. A recent study by Chim et al. (2023), using a stochastic volcanic forcing approach in a model  
160 with interactive sulfur chemistry and volcanic aerosols, showed that future volcanic forcing from 2015-2100 is very likely to  
161 exceed the 1850-2014 mean prescribed volcanic forcing used in CMIP6, with the median future forcing expected to be about  
162 twice that of the 1850-2014 mean. This finding raises questions about the degree to which a higher and sporadic future volcanic  
163 forcing would affect Antarctic ozone recovery.

165 In this study, we employ a plume-aerosol-chemistry-climate model with a stochastic volcanic forcing approach to simulate the  
166 effects of future volcanic sulfur injections on Antarctica and SH mid-latitude ozone recovery. Our stochastic future eruption  
167 scenarios resemble the statistical distribution of eruption frequency, latitude and sulfur mass in ice cores and satellite records.  
168 Based on multiple ozone recovery indicators we evaluate the effects of future volcanic eruptions on stratospheric ozone. Our  
169 model using stochastic scenarios indicates that future eruptions lead to delay in Antarctic ozone recovery assessed via changes  
170 in total column ozone, ozone mass deficit, and ozone hole area. We also conduct a composite analysis to show that the ozone  
171 response to volcanic sulfate aerosols over Antarctica and SH mid-latitudes is expected to decrease over this century. Given the  
172 inherent unpredictability of volcanic eruptions, the stochastic volcanic forcing approach offers insights into the uncertainties  
173 associated with future volcanic eruptions and their effects on the recovery of the Antarctic ozone layer.

## 174 2 Methods

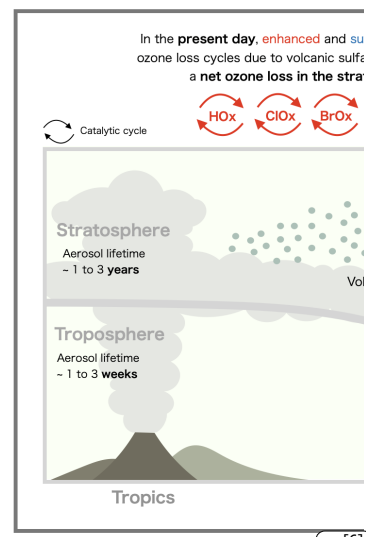
### 175 2.1 Model Setup

176 We use the UKESM simulations from Chim et al. (2023) and briefly summarise their design here. We first generate 1000  
177 stochastic future eruption scenarios from 2015 to 2100 by resampling eruptions recorded in bipolar ice cores and satellite  
178 observations over the past 11,500 years (Sigl et al., 2022; Carn, 2022). Our stochastic scenarios statistically resemble the  
179 eruption magnitude (in terms of volcanic SO<sub>2</sub> mass), eruption frequency, and eruption latitude of past volcanic eruptions.  
180 Based on the methodology developed in previous studies (Aubry et al., 2016; Bethke et al., 2017), we resample large-  
181 magnitude eruptions (defined as > 3 Tg of SO<sub>2</sub> mass injection) using volcanic emission datasets from both ice cores and

**Deleted:** Volcanic eruptions may also inject water vapour and volcanic halogen species into the stratosphere in addition to volcanic SO<sub>2</sub> and cause additional chemical ozone loss (Bobrowski et al., 2003; Pyle and Mather, 2009; Evan et al., 2023; Santee et al., 2024). Recent modelling studies demonstrate that the co-injection of volcanic sulfur and halogens into the stratosphere can lead to greater and prolonged ozone depletion compared to sulfur injections only (Klobas et al., 2017; Brenna et al., 2020; Ming et al., 2020; Staunton-Sykes et al., 2021). Klobas et al. (2017) used a 2D Chemistry Transport Model to simulate a Pinatubo-sized eruption with 7 Tg of SO<sub>2</sub> and co-injection of halogen in present-day and future background climates, which resulted in global mean column ozone loss up to 20% in both background climates. Staunton-Sykes et al. (2021) used the United Kingdom Earth System Model (UKESM) to demonstrate that a Samalás-like eruption (56 Tg of SO<sub>2</sub>) with (... [4]

**Formatted:** Subscript

**Deleted:** Klobas et al. (2017) emphasised the sensitivity of future ozone changes to a Pinatubo-like eruption with VSL bromine injection between 0 to 8 pptv, which can lead to changes in total column ozone over Antarctica between -3% and 3% under one future representative concentration pathway (i.e., RCP6.0). A more recent modelling study by Bednarz et al. (2022) found that VSL chlo (... [5]



**Deleted:** (... [6]

**Deleted:** highly unknown

**Deleted:** nature

**Deleted:** variability in

**Deleted:** forcing with volcanic

**Deleted:** only

277 satellite observations, and small-magnitude eruptions (defined as  $< 3$  Tg of  $\text{SO}_2$  mass injection) using satellite volcanic  
278 emission records only. We do not resample the emissions of volcanic halogen species and water vapour due to the lack of a  
279 comprehensive record of such species in the current ice-cores and satellite datasets. Consequently, we consider only the  
280 stratospheric volcanic  $\text{SO}_2$  mass in the resampling method.

281 We consider four scenarios as input for our future climate simulations: the low-end scenario (VOLC2.5, with 0.64 Tg of  $\text{SO}_2$   
282  $\text{yr}^{-1}$ ), the two median scenarios (VOLC50-1 and VOLC50-2, with 1.44 Tg of  $\text{SO}_2 \text{ yr}^{-1}$ ) and the high-end scenario (VOLC98,  
283 with 5.23 Tg of  $\text{SO}_2 \text{ yr}^{-1}$ ), each correspond to a scenario sampled near to the 2.5th, 50th, and 97.5th percentiles, respectively,  
284 of the ranked total sulfur mass of the 1000 stochastic scenarios. We perform simulations of the two median scenarios with  
285 small-magnitude eruptions only (VOLC50-1s and VOLC50-2s, with 0.64 and 0.57 Tg of  $\text{SO}_2 \text{ yr}^{-1}$ ) to evaluate the effects of  
286 small-magnitude eruptions. The results of the VOLC runs are compared against control simulations with constant volcanic  
287 forcing as in CMIP6 ScenarioMIP (CONST, with 0.77 to 0.86 Tg of  $\text{SO}_2 \text{ yr}^{-1}$  according to current volcanic emission records)  
288 and without explosive volcanic emissions (NOVOLC). All runs used the SSP3-7.0 scenario for anthropogenic forcings with  
289 simulation years between 2015 and 2100, with three ensemble members each. Fig. 1 shows the stratospheric sulfur burden  
290 globally, over the Antarctic, and SH mid-latitudes for the four selected stochastic scenarios (VOLC2.5, VOLC50-1, VOLC50-  
291 2, VOLC98).

Formatted: Subscript

Formatted: Font: 10 pt, Not Bold

Formatted: Font: 10 pt, Not Bold

Formatted: Font: Not Bold

Formatted: Font: 10 pt, Not Bold

Formatted: Font: 10 pt, Not Bold

Formatted: Font: Not Bold

Deleted: Table 1 summarises the model runs with the annual  $\text{SO}_2$  flux for each scenario used in this study.

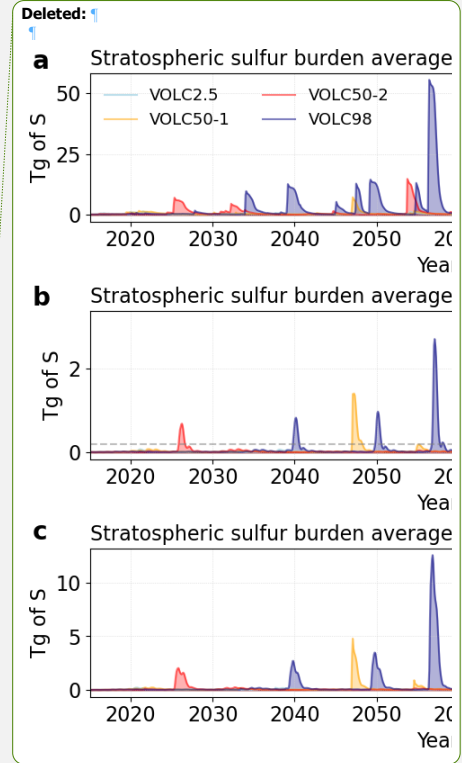
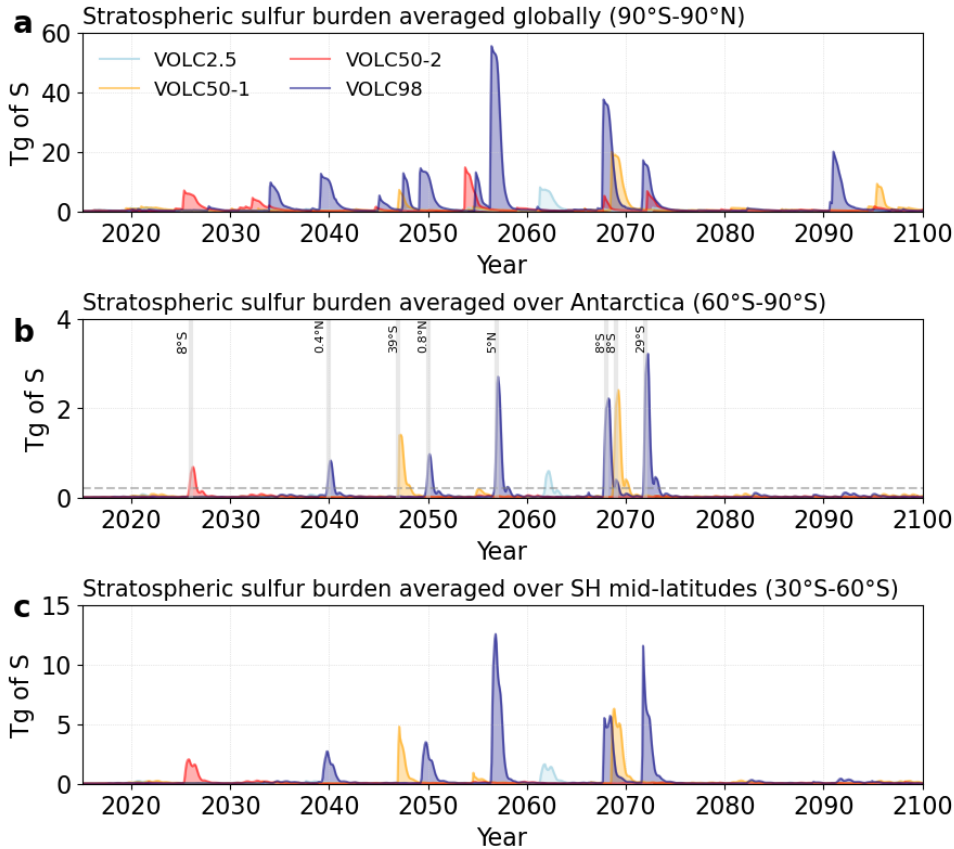
Deleted: 2

Deleted: Table 1. Model runs from Chim et al. (2023) used in this study. All runs used the SSP3-7.0 scenario for anthropogenic forcings with simulation years between 2015 and 2100, with three ensemble members each. The 1850-2014 mean  $\text{SO}_2$  flux for CMIP6/CCMI-2 volcanic forcing is estimated to have a range between 0.77 and 0.86 Tg of  $\text{SO}_2$  per year according to current volcanic emission records.<sup>4</sup>

Model runs

Model runs

... [7]



305  
 306 **Figure 1.** Stratospheric sulfur burden (in Tg of S) averaged (a) globally, (b) over Antarctica, and (c) over SH mid-latitudes from  
 307 2015 to 2100 for the four stochastic scenarios. The dotted line in panel (b) shows the stratospheric sulfur burden threshold of 0.2 Tg  
 308 of S, which is used to select eruptions for composite analysis. The injection latitudes of the selected eruptions are shown in panel (b).  
 309

Deleted: 2.

310 We employ the UKESM-VPLUME framework, which integrates the fully-coupled UK Earth System Model version 1.1 that  
 311 includes ocean-atmosphere interactions (UKESM1.1; Mulcahy et al., 2023) with a one-dimensional eruptive plume model  
 312 (Plumeria; Mastin, 2007, 2014). This framework allows for interactive stratospheric sulfur chemistry and volcanic sulfate  
 313 aerosols with plume injection heights consistent with background climate conditions, enabling the simulation of stratospheric  
 314 aerosol life cycle consistent with simulated future climate conditions. We evaluate the performance of UKESM1.1 in assessing

319 polar ozone concentrations by comparing the UKESM historical simulations with satellite observations (see Sect. 3.1). To  
320 evaluate the volcanic-induced ozone response in UKESM1.1, we perform a five-member ensemble of UKESM1.1 historical  
321 simulations from 1991 to 1993 to assess the model-simulated ozone response after the 1991 Mt. Pinatubo eruption. We inject  
322 10 Tg of SO<sub>2</sub> across 13 latitude bands between 0° and 15°N to allow the aerosols to be distributed in both hemispheres. [This  
323 injection approach is consistent with previous modelling studies using UM-UKCA and CESM \(Dhomse et al., 2014; Mills et  
324 al., 2016\)](#). We also perform a five-member ensemble without volcanic emissions as the control simulations.

325  
326 We perform future climate simulations under a high-end future shared socio-economic pathway (SSP3-7.0) from 2015 to 2100,  
327 with three ensemble members for each stochastic scenario. The emission projections in our simulations follow the ScenarioMIP  
328 experiment under SSP3-7.0, which do not include the emission of VSL chlorine and bromine compounds.

## 329 2.2 Ozone recovery indicators

330 We assess the effects of future eruptions on Antarctic ozone recovery by evaluating three ozone recovery indicators over the  
331 Antarctica (60°S to 90°S) and ~~SH~~ mid-latitudes (30°S to 60°S), including (1) total column ozone, (2) ozone mass deficit, and  
332 (3) ozone hole area. Total column ozone and ozone mass deficit have been used as ozone recovery indicators in previous  
333 studies to assess the recovery trend of ozone in the historical and future periods (Dhomse et al., 2018; de Laat et al., 2017;  
334 Stone et al., 2021). We assess the impact of volcanic forcing on Antarctic ozone return dates by comparing results of the VOLC  
335 runs versus the NOVOLC control run.

336 Total column ozone quantifies the ozone mass within the entire atmospheric column, measured in Dobson units (DU). The  
337 total column ozone recovery back to historical baseline (i.e., 1980 conditions) is a metric used by the UNEP/WMO Ozone  
338 Assessment Report (WMO, 2022). We use the 1978-1982 mean October total column ozone over Antarctica from UKESM1.1  
339 historical simulations (hereafter referred to as “1980 baseline”) to evaluate the return year of total column ozone concentrations  
340 relative to pre-industrial levels. We define the return year of the total ozone column as the last year of having an October mean  
341 total column ozone averaged over Antarctica that is lower than the 1980 baseline total column ozone value. We then ~~assess~~  
342 the delay in total column ozone recovery by comparing the return dates of VOLC runs with the control simulation NOVOLC.

343 Ozone mass deficit represents the deviation of the observed or model-simulated ozone mass from a reference value of the total  
344 ozone column over Antarctica. The value of 220 DU serves as a reference point frequently used to identify the depletion of  
345 Antarctic stratospheric ozone, as values less than 220 DU were not observed before 1979. In this study, we define two metrics  
346 for ozone mass deficit, one with a reference value of 220 DU and the second with a reference value of 175 DU. We define the  
347 return year of ozone mass deficit as the last year of having an October mean ozone mass deficit averaged over Antarctica that  
348 is lower than the 220 DU and 175 DU thresholds.

349 To quantify the uncertainty in return dates arising from interannual variability, we apply a Monte Carlo analysis to the ensemble  
350 mean of the October total column ozone and ozone mass deficit time series. Each series is first decomposed into a smoothed  
351 long-term trend and residuals. We then generate 1,000 realizations by resampling the residual variability and superimposing it  
352 on the trend. This approach yields a probabilistic distribution of return dates for crossing a specified ozone threshold, from  
353 which we report the median return year as well as the 5th to 95th percentile range.

354 Ozone hole area represents the spatial extent over the Antarctic where the total ozone column falls below a reference value.  
355 To define the presence or absence of an ozone hole in any given year, we use thresholds of total column ozone less than 220  
356 DU, 175 DU and 150 DU, respectively. We assess recovery trends of the October Antarctic ozone hole area by performing  
357 linear regression to evaluate the return dates, and compare against the control simulation NOVOLC.

Deleted: the

Deleted: cc

Deleted: -mean

361 **2.3 Composite analysis of ozone chemical loss**

362 We evaluate the chemical loss of Antarctic ozone using the stratospheric diagnostics developed by Lee et al. (2002). This  
363 method estimates the rate of odd oxygen ( $Ox = O_3 + O(^1P) + O(^1D)$ ) destruction for each catalytic cycle by determining the  
364 reaction rates of the rate-limiting steps. Under the assumption that  $[Ox] \approx [O_3]$ , the rate of odd oxygen loss is approximately  
365 equal to the rate of ozone loss for each catalytic cycle. We calculate the cumulative stratospheric ozone loss over Antarctica  
366 for the halogen cycles (i.e., the sum of ClOx and BrOx cycles), NOx cycle, and HOx cycle by integrating the monthly-mean  
367 ozone loss rate over time (from October to March) and altitude (up to 25 km). We calculate the cumulative stratospheric ozone  
368 loss over SH mid-latitudes by integrating the monthly-mean ozone loss rate up to 25 km for 12 months since the eruption  
369 month.

Formatted: Font: (Default) +Body (Times New Roman)

Formatted: Font: (Default) +Body (Times New Roman)

Deleted: the

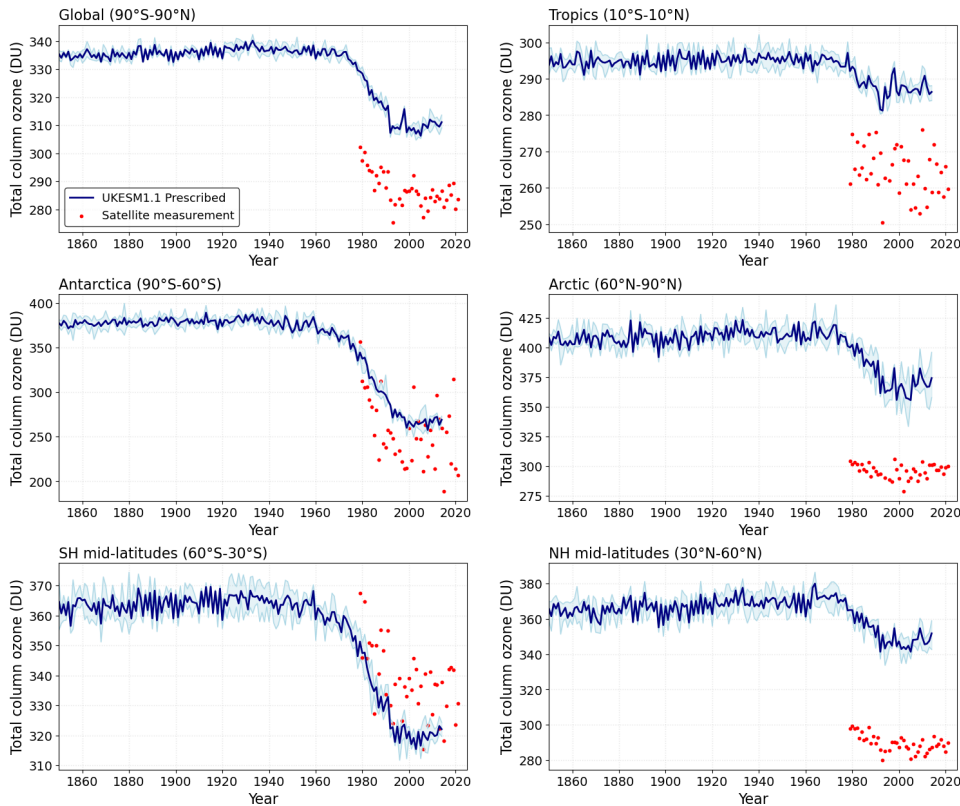
370 To evaluate the volcanic-induced ozone loss via catalytic cycles, we perform a composite analysis of the cumulative  
371 stratospheric ozone loss for selected eruptions. We identify 9 large-magnitude eruptions with stratospheric sulfur burden peaks  
372 greater than 0.2 Tg of S over the Antarctic (Fig. 2b) for performing composite analysis to evaluate the chemical changes via  
373 each catalytic cycle.

374 To assess the volcanic effects on Antarctic stratospheric ozone, we evaluate the relative differences in the chemical loss  
375 between the VOLC and NOVOLC runs. We calculate the cumulative stratospheric ozone loss anomaly relative to the control  
376 run (NOVOLC) for each catalytic cycle over Antarctica and SH mid-latitudes, using a 2-year window prior to the eruption as  
377 reference to compare with the 5-year post-eruption period. The peak ozone response (i.e., at year 0 since the eruption) for each  
378 selected eruption is normalised with the respective total sulfur mass and plotted against the eruption year for comparison.

379 **3 Results**

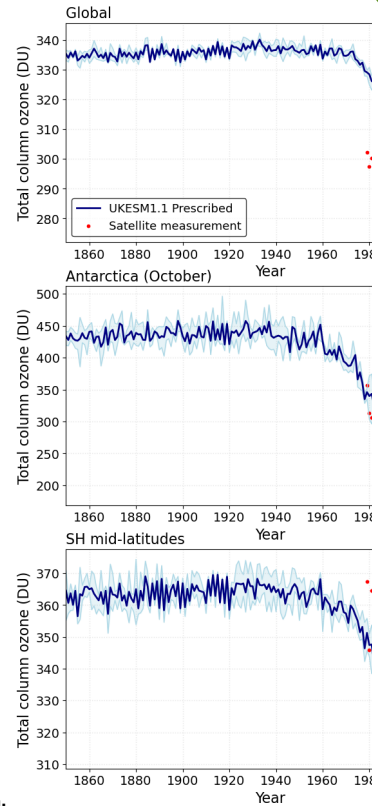
380 **3.1 Model Evaluation**

381 We assess the performance of UKESM in simulating ozone concentrations by comparing the total column ozone simulated by  
382 UKESM1.1 during the historical period (1850-2014) with satellite observations (Fig. 3). UKESM1.1 is the latest version of  
383 UKESM, incorporating several improvements compared to the previous model version, which reduced the cold bias in the  
384 historical global mean surface temperature by 50% (Mulcahy et al., 2023).



387 **Figure 2.** Annual mean total column ozone (in DU) averaged (a) globally (90°S to 90°N), over the (b) tropics (20°S to 20°N), (c)  
 388 Antarctica (60°S to 90°S), (d) Arctic (60°N to 90°N), (e) SH mid-latitudes (30°S to 60°S), and (f) NH mid-latitudes (30°N to 60°N). The  
 389 blue lines represent the UKESM historical simulations from 1850 to 2014, and the red markers represent satellite measurements  
 390 from 1978 to 2023. The blue shading shows the maximum and minimum values of the ensemble members.

391 Fig. 2 shows the total column ozone over different latitude bands simulated by UKESM1.1 with prescribed volcanic forcing  
 392 in the historical period from 1850 to 2014, along with satellite measurements from 1978 to 2023 obtained from the NASA  
 393 Ozone Watch (NASA Ozone Watch, 2023). UKESM1.1 tends to overestimate the global, tropical and NH mid- and high-  
 394 latitudes total column ozone as compared to satellite measurements. The total column ozone over SH mid-latitudes and  
 395 Antarctica shows good correspondence with satellite measurements. Nonetheless, UKESM has a high bias (+20%) in  
 396 stratospheric ozone compared to other CMIP6 models (Keeble et al., 2021), which stems from the bias over the tropics and



Deleted:

Deleted: 3

Deleted: , October mean

Deleted: , March mean

Deleted: 3

Formatted: Space After: 12 pt, Pattern: Clear (White)

Deleted: the

Deleted: in October

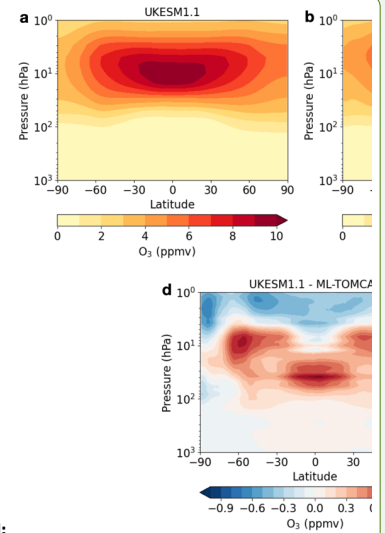
Northern Hemisphere (NH). Fig. S1 shows the comparison of the zonal mean ozone mass mixing ratio averaged from 2000 to 2014 for UKESM1.1, ML-TOMCAT merged 4-D ozone dataset (Dhomse et al., 2021; Dhomse and Chipperfield, 2023), and the CMIP6 multi-model mean (Keeble et al., 2021). We find that the zonal mean ozone distribution in UKESM1.1 in general agrees well with the ML-TOMCAT dataset. UKESM1.1 simulates higher ozone mass mixing ratio over the tropics and extratropical regions, lower ozone over Antarctic stratosphere from 1-10hPa, and higher ozone in the Antarctic lower stratosphere between 10-30 hPa compared to both ML-TOMCAT and the CMIP6 multi-model mean (Fig. S1d and e). This suggests that UKESM1.1 may overestimate lower stratospheric (10-30 hPa) ozone concentration over Antarctica relative to other CMIP6 models and ML-TOMCAT. UKESM1.1 also simulates higher total column ozone between 30°S and 60°N, and a deeper, more persistent Antarctic ozone hole compared to the CMIP6 multi-model mean (Fig. S2).

To assess the ozone response after volcanic eruptions in UKESM1.1, we performed a five-member ensemble of UKESM1.1 historical simulations for a case study of the 1991 Mt. Pinatubo eruption. We compared the UKESM1.1 model-simulated stratospheric aerosol optical depth (SAOD) and total column ozone with the Global Space-based Stratospheric Aerosol Climatology (GloSSAC) v2.2 dataset (Kovilakam et al., 2020) and the National Institute of Water and Atmospheric Research - Bodeker Scientific (NIWA-BS) filled total column ozone dataset v3.5.2 (Bodeker et al., 2021) to evaluate the model performance (Fig. 4). Our results show that UKESM1.1 simulates a higher SAOD over the tropics and NH (Fig. 4a and 4b), and the peak global mean SAOD value is 22% higher than that of GloSSAC (Fig. 4c). The ensemble-mean of the UKESM1.1-simulated total column ozone is able to capture total column ozone loss over Antarctic summer in 1991 and 1992, with a magnitude comparable to NIWA-BS total column ozone loss (Fig 4d to 4f). Although our simulations capture the magnitude of the Antarctic total column ozone response, the timing of ozone loss in 1991 does not match NIWA-BS. This discrepancy likely reflects differences between our free-running ensemble climatology and the 1991 atmospheric conditions, as our Pinatubo simulations are not nudged to observations. However, UKESM1.1 simulates a prolonged Antarctic total column ozone loss until spring when compared to NIWA-BS dataset (Fig. 4f).

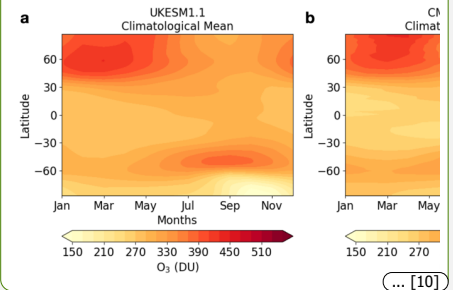
Deleted: [8]

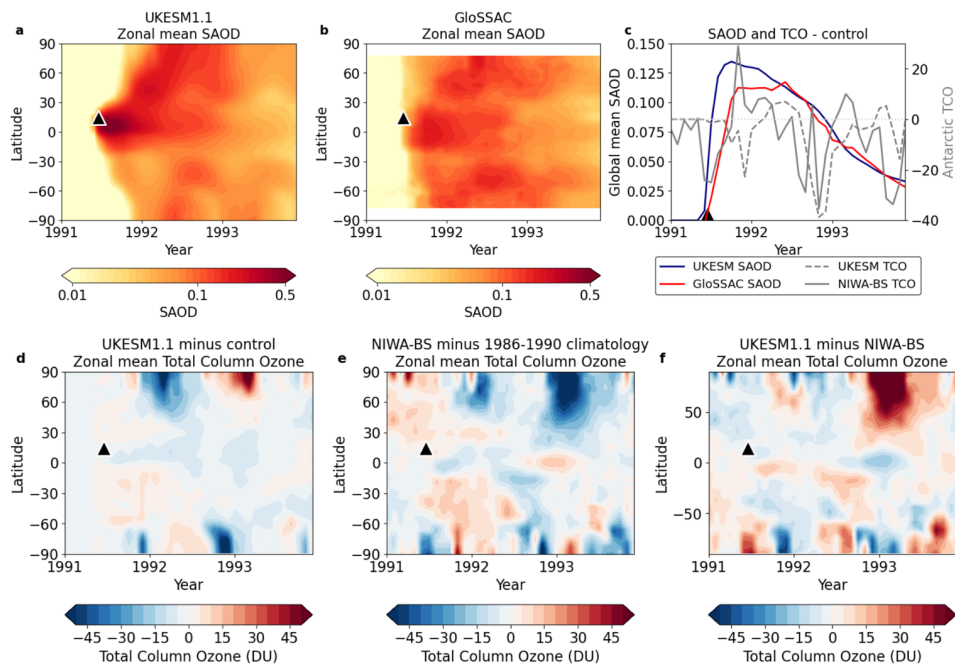
Deleted: lower stratosphere (10-30 hPa)

Deleted: a in climate projections than...relative to other CMIP6 models and ML-TOMCAT. Fig. 5 shows the climatological mean of total column ozone simulated by UKESM1.1 and the CMIP6 multi-model mean from Keeble et al. (2021). ...UKESM1.1 also simulates a...higher total column ozone between 30°S and 60°N,...and a deeper, and...ore persistent Antarctic ozone hole when ...ompared to the CMIP6 multi-model mean (Fig. S25



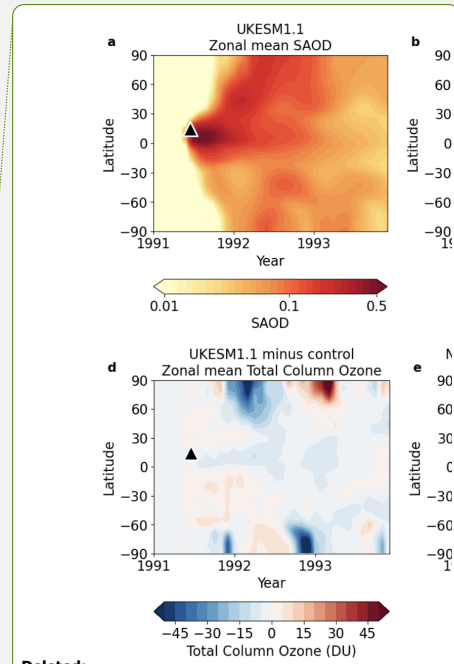
Deleted:  
Figure 4. Zonal mean ozone mass mixing ratio (ppmv), averaged from 2000-2014, for (a) UKESM1.1, (b) ML-TOMCAT, and (c) CMIP6 multi-model mean (MMM), (d) the difference between UKESM1.1 and ML-TOMCAT, and (e) the difference between UKESM1.1 and CMIP6 MMM. [10]





492 **Figure 3. Stratospheric aerosol optical depth (SAOD) and total column ozone responses following the 1991 Mt. Pinatubo eruption.**  
 493 (a,b) Zonal monthly mean SAOD from the UKESM1.1 simulation and GloSSAC. (c) Time series of global monthly mean SAOD  
 494 anomalies (UKESM1.1 relative to control and GloSSAC relative to 1986-1990 climatological mean) and Antarctic monthly mean  
 495 total column ozone anomalies (UKESM1.1 relative to control and NIWA-BS relative to 1986-1990 climatological mean). (d,e) Zonal  
 496 monthly mean total column ozone anomalies from UKESM1.1 (relative to control) and NIWA-BS (relative to 1986-1990  
 497 climatological mean). (f) Difference in total column ozone anomalies between UKESM1.1 and NIWA-BS (panel d minus e).

498 Fig. 4 presents our model-simulated daily size of the Antarctic ozone hole averaged over a 5-year period from 2015 to 2065  
 499 for one of our stochastic scenarios (VOLC50-1). Satellite observations from 1979 to 2022 suggest that the closure date of the  
 500 Antarctic ozone hole typically occurs between mid-November and late December (Copernicus Atmosphere Monitoring Service  
 501 (CAMS), 2023). However, the timing of the Antarctic ozone hole in our model results deviate significantly from historical  
 502 observations. Our model simulations show a considerably prolonged duration of the Antarctic ozone hole extending well into  
 503 February during the earlier decades of this century (Fig. 4). This discrepancy is attributed to the stratospheric cold bias of  
 504 UKESM over Antarctica, which is associated with a strong polar night jet and the strong downdraught of mesosphere air during  
 polar winter (Sellar et al., 2019), resulting in a stronger and more persistent polar vortex over Antarctica.



Deleted:

Deleted: 6

Deleted: 7

Deleted: 7

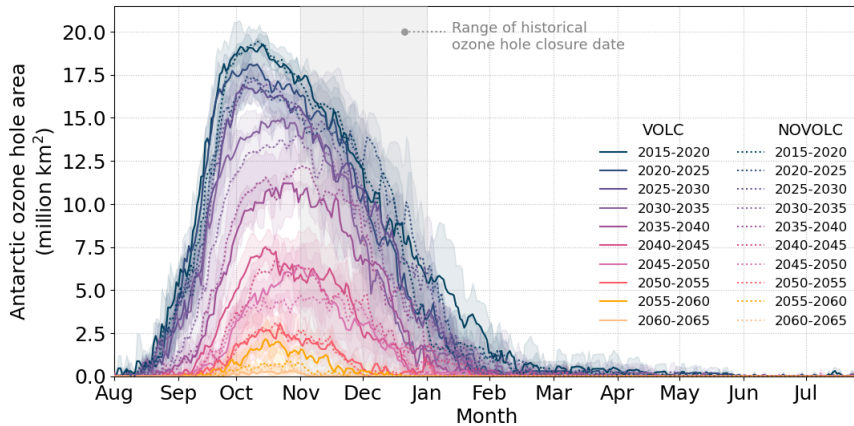


Figure 4. Daily size of the ozone hole area (5-year averaged) over Antarctica (60°S to 90°S, in million km<sup>2</sup>) for VOLC50-1 (solid lines) and NOVOLC (dotted lines). The colour shading shows the range of the maximum and minimum UKESM ensemble members. The grey shading shows the range of historical ozone hole (defined as area < 220 DU) closure date from satellite observations over 1979-2022 (CAMS, 2023).

Despite these limitations, we show that UKESM reproduces reasonably well the historical evolution of the October total ozone column (see Fig. 1c), when the ozone hole is at its deepest. This provides confidence in the model's ability to assess Antarctic ozone recovery by assessing the October-mean values of the ozone recovery indicators. The magnitude of Antarctic total column ozone response in our Pinatubo simulations also show a good agreement with observational datasets, suggesting that our estimates of relative impacts across different volcanic scenarios are robust. Since the stratospheric cold bias and strong winter polar vortex in UKESM (Sellar et al., 2019; Hall et al., 2021) likely hinder the transport of volcanic aerosols into the Antarctic stratosphere, we assess the ozone responses over both Antarctica and SH mid-latitudes.

### 3.2 Volcanic effects on Antarctic ozone recovery indicators

We use three ozone recovery indicators to assess the volcanic effects on Antarctic ozone return years, as summarised in Table 1. We find that the return year of ozone mass deficit to 220 DU threshold is delayed by 0 to 2 years for the low-end and median future scenarios (VOLC2.5 and VOLC50, Table 1), and 5 years for a high-end future eruption scenario (VOLC98, Table 1). Although some stochastic scenarios indicate a later median return year, the overlap in uncertainty ranges suggests that the delay is not distinguishable from internal variability (Table 1). On the other hand, the return year of ozone mass deficit to the 175 DU threshold ranges between 0 to 5 years across the stochastic scenarios.

Table 1. Return years of the ozone recovery indicators for Antarctic October-mean values, including total column ozone (median return year relative to the model 1980 baseline), the Antarctic October-mean ozone mass deficit (median return year relative to the 220DU and 175DU thresholds), and the Antarctic October-mean ozone hole area (220 DU threshold). Numbers in brackets indicate the 5th to 95th percentile uncertainty range from the Monte Carlo uncertainty analysis. For the ozone hole area recovery trend, the uncertainty range corresponds to the spread across the three ensemble members.

Deleted: 7

Deleted: ¶

Formatted: Font: 10 pt, Not Bold

Deleted: 2

Deleted: 2

Deleted: 2

Deleted: natural

Deleted: 2

Deleted: 2

Indicator	NOVOLC	VOLC2.5	VOLC50-1	VOLC50-1s	VOLC50-2	VOLC50-2s	VOLC98
<b>Total ozone column</b>	2066 (2062-2072)	2065 (2063-2074)	2064 (2058-2072)	2068 (2059-2075)	2069 (2062-2075)	2069 (2062-2077)	2071 (2066-2074)
<b>Ozone mass deficit (220 DU)</b>	2062 (2054-2065)	2064 (2059-2066)	2060 (2050-2069)	2060 (2052-2062)	2062 (2051-2064)	2062 (2053-2064)	2068 (2047-2073)
<b>Ozone mass deficit (175 DU)</b>	2038 (2022-2041)	2041 (2024-2044)	2038 (2022-2042)	2039 (2023-2043)	2044 (2036-2046)	2039 (2030-2041)	2041 (2030-2044)
<b>Ozone hole area (220 DU)</b>	2058 (2058-2059)	2058 (2056-2060)	2059 (2058-2060)	2059 (2059-2060)	2059 (2058-2060)	2059 (2058-2059)	2061 (2060-2062)

561  
562  
563  
564  
565  
566  
567  
568  
569  
570  
571  
572

Figure 5a and 5b shows the October-mean ozone mass deficit over Antarctica with 220 DU and 175 DU thresholds respectively, shown as 30-year and 3-year moving means. The 3-year moving mean reveals substantial interannual variability in ozone mass deficit across scenarios, driven by individual eruptions and internal variability. When smoothed with a 30-year moving mean to show longer-term trends, all stochastic scenarios consistently exhibit higher ozone mass deficit compared to NOVOLC prior to their respective return years (Fig. 5a and 5b). The relative contribution of volcanic effects to ozone mass deficit in year 2030 ranges between 5.7% to 8.7% (0.7 million tonnes to 1.0 million tonnes) using a 220 DU threshold, and 8.9% to 23.0% (0.2 million tonnes to 0.5 million tonnes) using a 175 DU threshold across the stochastic scenarios (Fig. 5a and 5b). The median return years for ozone mass deficit with a 220 DU threshold are the same for the VOLC50 scenarios and their respective runs with small-magnitude eruptions only (VOLC50-1s and VOLC50-2s). For the 175 DU threshold, VOLC50-2s shows an earlier return by 5 years for both the median and 5th to 95th percentile ranges as compared to VOLC50-2, while VOLC-501s shows a 1-year delay in return year as compared to VOLC50-1.

- Deleted: 8
- Deleted: 8
- Deleted: natural climate
- Deleted: Regardless of the threshold chosen,
- Deleted: of our
- Deleted: have
- Deleted: when averaged with a 30-year moving mean
- Deleted: 8
- Deleted: 8
- Deleted: 8
- Deleted: 8

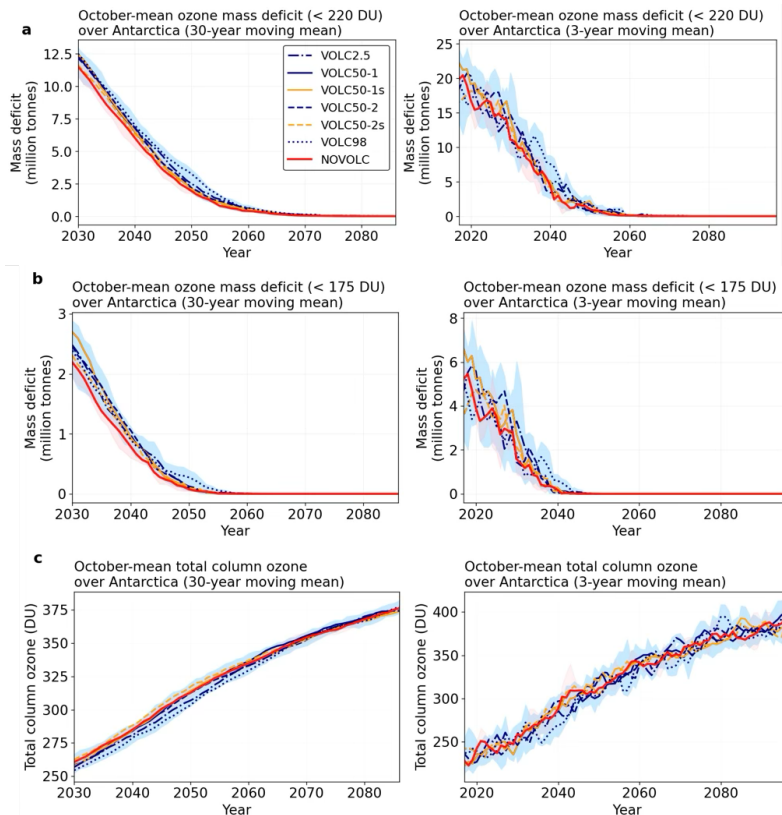
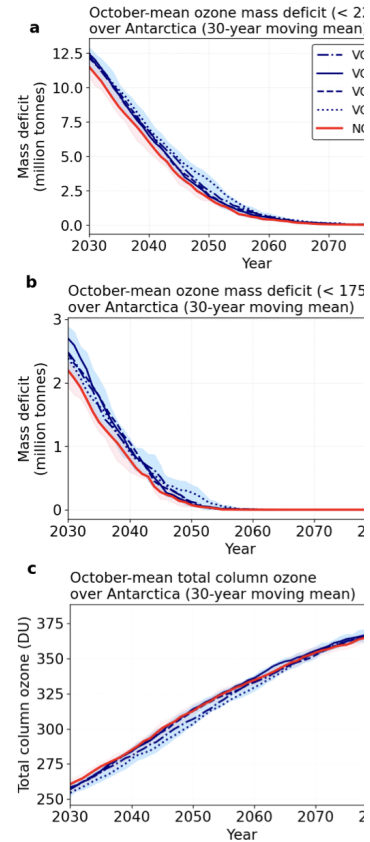


Figure 5. October-mean ozone recovery indicators over Antarctica. (a) Ozone mass deficit using the 220 DU threshold (in million tonnes), (b) ozone mass deficit using the 175 DU threshold (in million tonnes), and (c) total column ozone (in DU). The left column shows the values applied with a 30-year moving mean, and the right column shows the values applied with a 3-year moving mean.

Figure 5c shows the time series of the October-mean Antarctic total column ozone. Compared to the NOVOLC run, our stochastic scenarios show a 0.5% to 2.8% (1.5 DU to 8 DU) lower Antarctic total column ozone averaged over 2030 to 2050, which lasts until around 2060s for some stochastic scenarios. The greater volcanic-induced impact on ozone loss in the near-term is likely due to the higher chlorine concentrations in the atmosphere as compared to the later decades. In our model and without considering future volcanic eruptions, Antarctic total column ozone returns to its 1980 baseline in 2066 (range: 2062-2072, NOVOLC). Among all the simulated stochastic scenarios, only the median scenario VOLC50-2 and the high-end scenario VOLC98 show delays in the Antarctic total column ozone return date, by 3 years and 5 years respectively. One of the median scenarios with small-magnitude eruptions only (VOLC50-1s) has a 4-year delay in the median return date of total



Deleted:

Formatted: English (US)

Deleted: 8

Deleted: 8

Deleted: T

Deleted: only

Deleted: 2

Deleted: also

604 column ozone compared to VOLC50-1, while the other median stochastic scenario (VOLC50-2) has the same return year as  
605 the scenario with small-magnitude eruptions only (VOLC50-2s).

607 We also examine the responses of the annual mean total column ozone globally and over SH mid-latitudes (Figure S3a and  
608 S3b). Our results show that volcanic sulfate aerosols induce a reduction of 0.4% to 0.6% (1.2 DU to 1.9 DU) in total column  
609 ozone over SH mid-latitudes, and 0.3% to 0.5% (0.9 DU to 1.6 DU) globally, relative to the NOVOLC simulation for the  
610 period 2030–2086. The magnitude of response in global and SH mid-latitude total column ozone is consistently negative  
611 throughout this century and comparable to or slightly greater than that over Antarctica (+0.1% to -0.5%, Fig. S3d), where the  
612 response shows greater variability.

614 Figure 6 shows the October-mean Antarctic ozone hole area for the VOLC and NOVOLC runs, with the zonal-mean  
615 stratospheric aerosol optical depth of the respective VOLC runs shown in each panel. To assess the return year of the Antarctic  
616 ozone hole area, we assess the recovery trend of the Antarctic ozone hole area. We find that the recovery of the Antarctic  
617 ozone hole area back to 220 DU is delayed by 1 to 3 years, except for the VOLC2.5 scenario (Table 1). Small-magnitude  
618 eruptions (VOLC50-1s and VOLC50-2s) have no impact on the median return dates of the Antarctic ozone hole area. The  
619 longer delay in the VOLC98 scenario can be attributed to the occurrence of a large-magnitude tropical eruption in 2056  
620 emitting 114 Tg of SO<sub>2</sub> (Fig. 1), which results in a high SAOD over Antarctica and an Antarctic October ozone hole area of 5  
621 million km<sup>2</sup> relative to NOVOLC (Fig. 6). Although we see a delay in the recovery of the Antarctic ozone hole area in most  
622 of the VOLC scenarios for a 220 DU threshold, our simulation results also show that the Antarctic ozone hole area is highly  
623 variable between ensemble members. We are not able to perform robust statistical tests due to the limited number of ensemble  
624 members. We also examine the Antarctic ozone hole area recovery under a lower total column ozone threshold of 175 DU and  
625 150 DU. The Antarctic ozone hole area recovery is delayed by 1 year in most VOLC scenarios except for VOLC2.5 for a 175  
626 DU threshold, and there is no delay in return date in all scenarios for a 150 DU threshold (Supplementary Fig. S4 and S5).

Deleted: than

Deleted: produces a 3-year delay, indicating that small eruptions have little impact on Antarctic total column ozone recovery.

Deleted: the

Deleted: 1

Deleted: 1

Deleted: 5

Deleted: 8

Deleted: 9

Deleted: 3.0

Deleted: the

Deleted: e

Deleted: smaller

Deleted: a

Deleted: c

Deleted: .

Deleted: 9

Deleted: (Table 2)

Deleted: 2

Deleted: 9

Deleted: 2

Deleted: 3

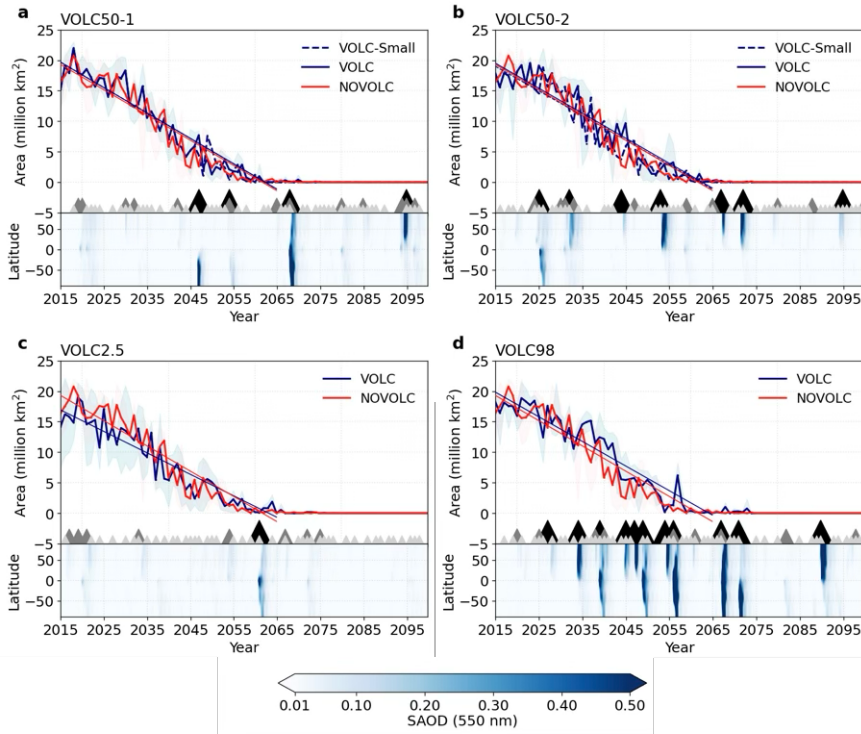
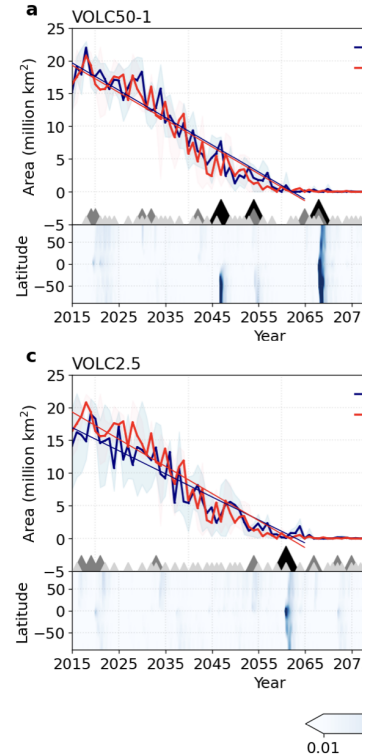


Figure 6. October-mean ozone hole area (in million km<sup>2</sup>) averaged over Antarctica for (a) VOLC50-1, (b) VOLC50-2, (c) VOLC2.5, and (d) VOLC98. The blue lines show the ensemble mean values and the linear regression for each VOLC scenario, the red lines show the ensemble mean values for NOVOLC, and the shading shows the values of the maximum and minimum values across the ensemble members. The triangles refer to the occurrence of eruptions in each stochastic scenario: the black triangles refer to eruptions with > 3 Tg of SO<sub>2</sub> injection, the grey triangles refer to eruptions with 1 to 3 Tg of SO<sub>2</sub> injection, and the light grey triangles refer to eruptions with 0.1 to 1 Tg of SO<sub>2</sub> injection. The lower panel shows the zonal mean stratospheric aerosol optical depth at 550 nm for the four VOLC runs.

### 3.3 Chemical changes in the Antarctic and SH mid-latitudes lower stratosphere

To assess the volcanic effects on the chemical loss of ozone, we select 9 large-magnitude eruptions with stratospheric sulfur burden > 0.2 Tg of S over Antarctica for composite analysis (Figure 1b). Fig. 7a shows the composite analysis results of the cumulative stratospheric ozone loss anomaly relative to NOVOLC over Antarctic and SH mid-latitudes for each catalytic cycle. A positive value indicates a net ozone loss via the catalytic cycle, while a negative value indicates a net ozone gain. Our



Deleted:

Deleted: 9

Deleted: 9

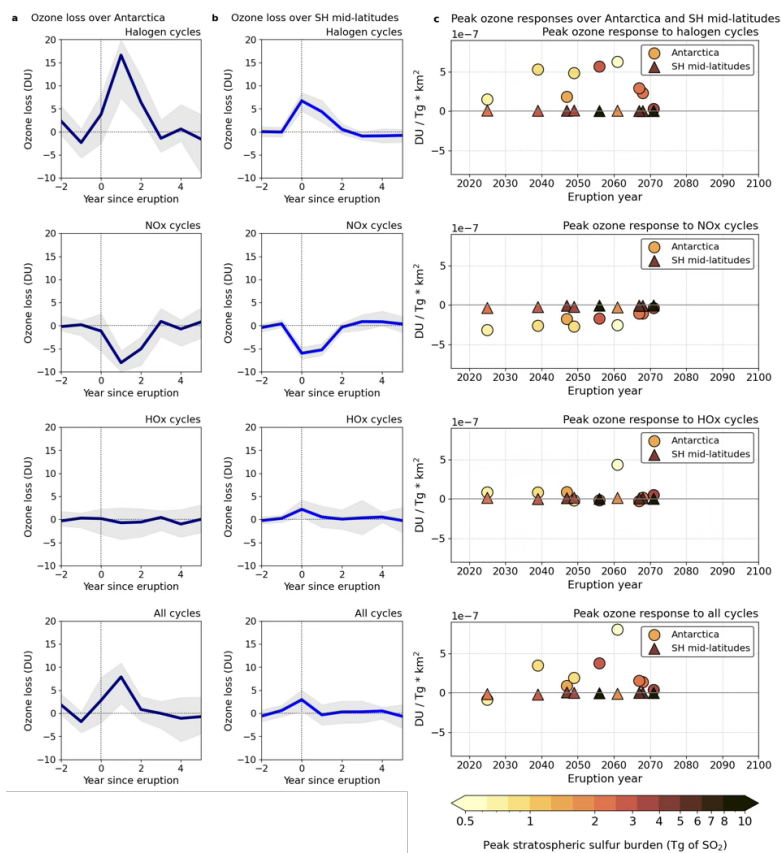
... [11]

Deleted: 10

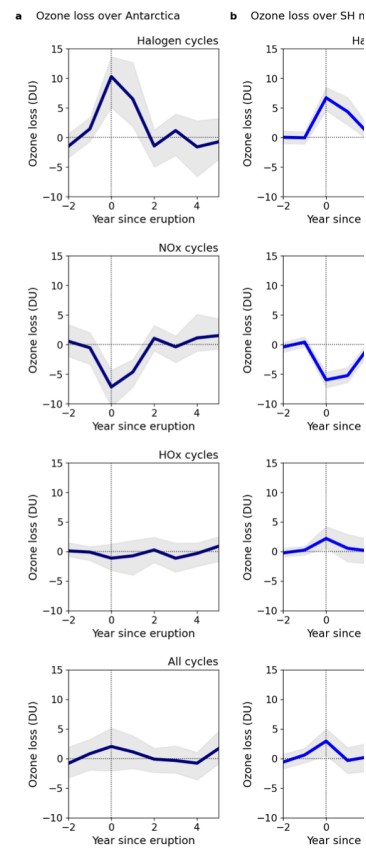
672 analysis shows a net ozone loss via halogen cycles at year zero after volcanic eruptions, and a net ozone increase via NOx  
 673 cycle over Antarctica and SH mid-latitudes (Fig. 7a and 7b). The volcanic-induced ozone response via halogen and NOx  
 674 is stronger over Antarctica than the SH mid-latitudes, as shown in Figure 10a. Stratospheric volcanic sulfate aerosols catalyse  
 675 the release of active chlorine from reservoir species via heterogeneous chemistry, forming ClOx (Fig. S6). This enhances  
 676 stratospheric ozone loss via halogen cycles over Antarctica and SH mid-latitudes (Figure S8 and S9). The sulfate aerosols also  
 677 catalyse the hydrolysis of N<sub>2</sub>O<sub>5</sub> (Fig. S7), suppressing the NOx-catalysed ozone loss for 1 to 2 years after the eruption (Fig.  
 678 S8 and S9).

**Deleted:** 10... and 710...). The volcanic-induced ozone response via halogen and NOx cycles is stronger over Antarctica than the SH mid-latitudes, as shown in Figure 10a. Stratospheric volcanic sulfate aerosols catalyse the release of active chlorine from reservoir species via heterogeneous chemistry, forming ClOx (Fig. S64.... This enhances stratospheric ozone loss via halogen cycles over Antarctica and SH mid-latitudes (Figure S86... and S97.... The sulfate aerosols also catalyse the hydrolysis of N<sub>2</sub>O<sub>5</sub> (Fig. S75...., suppressing the NOx-catalysed ozone loss for 1 to 2 years after the eruption (Fig. S86... and S97

... [12]



680 **Figure 7.** Composite analysis of the cumulative stratospheric ozone loss (up to 25 km) relative to NOVOLC for the 9 selected  
 681 eruptions (a) over Antarctica, integrated by time from August to the following July, and (b) SH mid-latitudes, cumulative loss for  
 682



**Deleted:**

**Deleted:** 10... Composite analysis of the cumulative stratospheric ozone loss (up to 25 km) relative to NOVOLC for the 9 selected eruptions (a) over Antarctica, integrated by time from October to March

... [13]

**Deleted:** the

12 months after the onset of each eruption. Year 0 denotes the year of eruption. The shaded region shows the range of the first and third quartiles. (c) Peak ozone response of the selected eruptions to halogen cycles, NO<sub>x</sub> cycle, HO<sub>x</sub> cycle, and all cycles (halogen + NO<sub>x</sub> + HO<sub>x</sub>) over Antarctica (circles) and SH mid-latitudes (triangles). The values are normalised with the respective peak stratospheric S burden for each eruption and total area over Antarctica and SH mid-latitudes, respectively.

Fig. 7c shows the peak ozone response (i.e., the response at year 0 or 1 of the composite analysis) via the catalytic cycles, normalised by the respective peak stratospheric sulfur burden and total area over Antarctica and SH mid-latitudes. The normalised peak ozone response exhibits a decreasing trend with eruption year for both regions and is stronger over Antarctica than the SH mid-latitudes (Fig. 7a and 7b). However, the overall magnitude of ozone response, summing all catalytic cycles, is comparable between the Antarctica and SH mid-latitudes (Fig. 7c). Although we see clear decreasing trends in ozone response over both regions, we are unable to identify the shift in the ozone chemistry response due to a lack of large-magnitude eruptions with > 0.2 Tg of S over Antarctica after 2070 in these simulations.

#### 4 Discussion

Using a plume-aerosol-chemistry-climate model UKESM-VPLUME with an improved stochastic volcanic forcing, we assess the effect of future volcanic eruptions with sulfur injections on Antarctic and SH mid-latitude ozone recovery by evaluating the October-mean values of three ozone recovery indicators. We find that the extent of the delay in Antarctic ozone return dates depends on the eruption timing, latitude and aerosol distribution in the stochastic scenarios, with two scenarios showing delays in ozone mass deficit of 2 years (VOLC2.5) and up to 5 years (VOLC98) with a 220 DU ozone threshold (Table 1). If we use a lower ozone threshold of 175 DU, the relative effect of volcanic eruptions on ozone mass deficit can be up to 23% in 2030 for a high-end future scenario (Fig. 5b). For the 175 DU threshold, VOLC50-2 shows the longest delay (6 years), while VOLC2.5 and VOLC98 both show 3-year delays, and VOLC50-1 has the same return year as NOVOLC. The apparent inconsistencies in the delays of recovery across scenarios arise from the different recovery timelines, which is due to differences in the timing of volcanic eruptions across scenarios, as well as varying sensitivities of the two ozone mass deficit thresholds. The recovery for the 175 DU threshold is much faster (median year of 2038 in NOVOLC) than the 220 DU threshold (median year of 2062 in NOVOLC), making each metric sensitive to eruptions occurring at different times. For instance, VOLC2.5 and VOLC98 both have large-magnitude eruptions with SH aerosol distribution before 2062, thus showing greater delay in return years for the 220 DU threshold. VOLC50-2 shows the longest delay for the 175 DU threshold because it has higher SH SAOD than VOLC2.5 and VOLC98 before 2038 (Fig. 6). In contrast, the first large-magnitude eruption in VOLC50-1 occurs in 2047, after the 175 DU threshold recovery year, and thus showing no delay for this metric.

We also show that future scenarios with small-magnitude eruptions only (VOLC50-1s and VOLC50-2s) have no effect on the return years of Antarctic ozone mass deficit with a 220 DU threshold, but have a mixed effect on the recovery of deeper ozone holes at the 175 DU threshold. One of the scenarios with small-magnitude eruptions only (VOLC50-2s), which has the lowest annual SO<sub>2</sub> flux (0.57 Tg SO<sub>2</sub> yr<sup>-1</sup>), shows earlier recovery by 5 years for the 175 DU threshold metric, while the other small-magnitude scenario (VOLC50-1s) shows a 1-year delay compared to VOLC50-1 (Table 1). This suggests that ozone recovery timing is primarily governed by large-magnitude eruptions, with small-magnitude eruptions playing a secondary role. However, the large uncertainty ranges and overlapping values in the return years between VOLC and NOVOLC scenarios reflect substantial internal variability between ensemble members: this highlights that recovery projections should be interpreted as ranges rather than median values alone. Our simulations are also limited by the number of ensemble members. Future modelling experiments with larger ensemble sizes would further quantify the uncertainty in volcanic effects on ozone recovery and distinguish between volcanic forcing effects and internal variability.

Deleted:

Deleted: 10... shows the peak ozone response (i.e., the response at year 0 or 1 of the composite analysis) via the catalytic cycles, normalised by the respective peak stratospheric sulfur burden and total area over Antarctica and SH mid-latitudes. The normalised peak ozone response exhibits a decreasing trend with eruption year for both regions and is stronger over Antarctica than the SH mid-latitudes (Fig. 710... and 710...). However, the overall magnitude of ozone response, summing all catalytic cycles, is comparable between the Antarctica and SH mid-latitudes (Fig. ...710 ... [14]

Deleted: d

Deleted: 2... If we use a lower ozone threshold of 175 DU, the relative effect of volcanic eruptions on ozone mass deficit can be up to 23% in 2030 for a high-end future scenario (Fig. 58 ... [15]

Formatted: Font colour: Text 1

Formatted

Deleted: and

Deleted: recovers

Formatted: Font colour: Text 1

Formatted

Deleted: For the 175 DU threshold,

Formatted

Deleted: show

Formatted

Deleted: One of the volcanically quiescent scenarios ...VOLC50-2s), which has the lowest annual SO<sub>2</sub> flux (0.57 Tg SO<sub>2</sub> yr<sup>-1</sup>), shows earlier recovery by 5 years for the 175 DU threshold metric, while the other small-magnitude scenario (VOLC50-1s) shows a 1-year delay compared to its parent scenario...VOLC50-1 (Table 1). This suggests that ozone recovery timing is primarily governed by large-magnitude eruptions, with small-magnitude eruptions playing a secondary role. However, the large uncertainty ranges and overlapping values in the return years between VOLC and NOVOLC scenarios reflect substantial natural ... [20]

Formatted: Font colour: Text 1

Deleted: Given...ur simulations are also our ... [21]

Deleted: and the substantial uncertainty range in the return dates, these results should be interpreted cautiously... Future modelling experiments with larger ensemble sizes would better ... [22]

Formatted: Font colour: Text 1

Deleted: impacts

Formatted: Font colour: Text 1

Formatted: Font colour: Text 1

Deleted: climate

827 In terms of the total column ozone, we find a delay of up to 5 years in the high-end volcanic scenario (VOLC98), which  
828 includes volcanic eruptions with large stratospheric sulfur burdens and SAOD over Antarctica between the years 2055 and  
829 2065 (Fig. 4 and 5). Our results show that an adopted large-magnitude tropical eruption in the year 2056 in the VOLC98  
830 scenario, with an Antarctic sulfur burden of 2.7 Tg of S, leads to an Antarctic ozone hole exceeding 5 million km<sup>2</sup> in October  
831 (Fig. 6d). This occurs despite the Antarctic ozone column being otherwise close to returning to 1980 values in the 2050s. The  
832 simulated ozone hole is comparable in size to that caused by the 2015 Calbuco eruption, which emitted around 0.4 Tg of SO<sub>2</sub>  
833 and resulted in an October ozone hole of about 4.5 million km<sup>2</sup> larger (Solomon et al., 2016). The comparable ozone hole size  
834 is attributable to the substantially higher stratospheric chlorine loading in 2015 compared to that projected for the mid-21st  
835 century. These findings demonstrate that future eruptions with significant volcanic sulfur injections have the potential to cause  
836 large Antarctic ozone holes in the middle of this century according to our simulations.

Deleted: 1

Deleted: 2

Deleted: 8

Deleted: 9

837 Our results differ from with the findings of Naik et al. (2017), another previous modelling study that assessed the effects of  
838 future volcanic eruptions on stratospheric ozone recovery in climate projections. Naik et al. (2017) use a prescribed constant  
839 future volcanic forcing equivalent to the 1860-1999 mean volcanic forcing to evaluate stratospheric ozone responses in climate  
840 projections using the GFDL-CM3 model under the RCP4.5 and RCP8.5 scenarios. Their model results suggest that an  
841 enhanced volcanic sulfate aerosol burden does not affect Antarctic ozone column return dates but leads to an earlier recovery  
842 of global stratospheric ozone. The disagreement between Naik et al. (2017) and our study potentially arises from differences  
843 in forcing magnitude, model responses and chemistry representations between GFDL-CM3 and UKESM. For instance, the  
844 ClO/Cly ratio at 50°N in Naik et al. (2017) is a factor of 4 lower than observations on 22 March 1992, following the 1991 Mt.  
845 Pinatubo eruption (Fahey et al., 1993), suggesting that the GFDL model may not adequately capture the response of halogen  
846 chemistry. In addition, the UKESM model version used in our study has limited heterogeneous reactions, whereas a recent  
847 study by Ming et al. (2020) used a new heterogeneous scheme in UKESM with eight additional reactions, producing a better  
848 match with the observed total column ozone over Antarctica. Beyond differences in model chemistry responses, the contrasting  
849 results are likely stemming from the experimental design (prescribed versus interactive volcanic forcing) and different future  
850 emission scenarios used (RCP versus SSP). These differences hinder direct comparison between the two studies. Future model  
851 comparison studies using consistent future emission scenarios and volcanic forcing magnitudes are necessary to assess the  
852 projected ozone responses to volcanic eruptions across different models.

Deleted: 1

Deleted: contrast

854 Our composite analysis of cumulative stratospheric ozone response reveals a net ozone loss for the 9 selected large-magnitude  
855 eruptions (Fig. 7c). The stratospheric ozone response to volcanic eruptions is sensitive to the amount of aerosol mass  
856 transported into the polar vortex (Fig. 1). Our results show a linear decreasing trend of peak ozone response after large-  
857 magnitude eruptions. However, due to the lack of large-magnitude eruptions after 2070 with high sulfur burden over Antarctica  
858 in our stochastic scenarios, we do not see a clear shift from net stratospheric ozone loss to production over Antarctica. We  
859 expect that eruptions occurring after year 2070 will eventually lead to a net ozone gain instead of ozone loss. Such shifting in  
860 the chemistry will affect the future ozone recovery trend. Our findings indicate that even a small-magnitude eruption in 2092,  
861 with a SO<sub>2</sub> injection mass of less than 3 Tg of SO<sub>2</sub> and an Antarctic sulfur burden as low as 0.08 Tg of S, can lead to a small  
862 net ozone loss over Antarctica (Fig. S8). The stratospheric ozone response to volcanic eruptions is also influenced by  
863 stratospheric dynamics. However, due to the coupled nature of our model simulations, we are unable to isolate and quantify  
864 the dynamical component of the ozone response. Furthermore, the stochastic nature of our scenarios and the limited model run  
865 length constrain our ability to identify the timing of the shift in stratospheric ozone response to volcanic eruptions, as the shift  
866 in the ozone chemistry may occur after 2100. Nonetheless, our study demonstrates that the composite analysis of the  
867 stratospheric ozone loss via catalytic cycles is a valuable tool for evaluating the chemical response of stratospheric ozone to  
868 volcanic eruptions.

Deleted: 10

Deleted: 2

Deleted: 6

878 Although our study primarily focuses on the ozone response over Antarctica and SH mid-latitudes, volcanic eruptions can also  
879 induce significant changes in ozone concentrations over the Arctic and NH mid-latitudes (Fig. S3c, S10 and S11). Composite  
880 analysis of 15 selected eruptions (with a stratospheric sulfur burden exceeding 0.5 Tg of S over the NH mid-latitudes) reveals  
881 substantial net ozone loss of 9 DU over the Arctic (interquartile range: 18 DU to 2 DU) and 2 DU loss over the NH mid-  
882 latitudes (interquartile range: 6 DU to 3 DU) (Figures S12). However, the ozone response over these regions exhibits greater  
883 uncertainties and variability compared to the SH. The limited ensemble size in this study constrains our ability to draw robust  
884 conclusions regarding the NH ozone response. Furthermore, the occurrence of multiple volcanic eruptions between 2040 and  
885 2060 in the VOLC98 scenario (Fig. 1) may introduce biases in the composite analysis, as the overlapping ozone responses  
886 from these closely timed eruptions could potentially interfere with one another (Fig. S12). Consequently, while our findings  
887 highlight the potential for volcanic eruptions to impact stratospheric ozone recovery over polar regions, additional research  
888 with larger ensemble simulations is necessary to more comprehensively characterise the ozone response over the Arctic and  
889 NH mid-latitudes.

890 We acknowledge that UKESM1.1 exhibits a stratospheric cold bias and excessively strong polar vortex that leads to prolonged  
891 ozone depletion over Antarctica (Fig. 4). The comparison of the UKESM1.1 simulation with ML-TOMCAT shows that the  
892 climatological mean of UKESM1.1 overestimates lower stratospheric ozone loss over Antarctica and SH mid-latitudes. Due  
893 to these model biases, our results likely overestimate the cumulative ozone loss over Antarctica and SH mid-latitudes.  
894 However, the relative volcanic effects on ozone in our simulated scenarios remain robust. In addition, our stochastic scenarios  
895 include stratospheric volcanic SO<sub>2</sub> emissions only, but not volcanic halogen species, water vapour and VSL chlorine and  
896 bromine compounds, which affect stratospheric ozone recovery. Klobas et al. (2017) emphasised the sensitivity of future ozone  
897 changes to a Pinatubo-like eruption with VSL bromine injection between 0 to 8 pptv, which can lead to changes in total column  
898 ozone over Antarctica between -3% and 3% under one future representative concentration pathway (i.e., RCP6.0). Although  
899 VSL chlorine has a small contribution to total stratospheric chlorine (about 3%) between 2010 to 2019 (Bednarz et al., 2022),  
900 the increasing emission of VSL chlorine highlights the potential importance of its impact on future ozone changes. By not  
901 accounting for VSL species in our simulations, we likely underestimate the full magnitude of volcanic impacts on ozone  
902 recovery. The lack of comprehensive historical records on volcanic halogen emissions, the variability in halogen injections  
903 across different eruptions, and the uncertainties in future VSL halogenated compounds emissions make it challenging to project  
904 future stratospheric halogen loadings using our stochastic approach. Therefore, our model-simulated effects on ozone represent  
905 a lower bound of the potential effects of future volcanic eruptions on ozone depletion. We anticipate that including volcanic  
906 halogen, water vapour, and VSL chlorine and bromine emissions in our stochastic scenarios would likely result in further  
907 delays to Antarctic and SH mid-latitude ozone recovery. It is essential to improve current volcanic halogen emission datasets  
908 and proxy records, and account for the emission of halogenated VSL compounds to better assess the impact of future volcanic  
909 eruptions on stratospheric ozone recovery.

910  
911 Our model experiments use a high-end future anthropogenic emission scenario (SSP3-7.0) which has high future methane  
912 emissions (Meinshausen et al., 2020). Previous studies showed that stratospheric ozone responses to volcanic eruptions are  
913 sensitive to the background anthropogenic greenhouse gas emissions (Naik et al., 2017; Klobas et al., 2017). For instance,  
914 Klobas et al. (2017) demonstrate that ozone depletion after volcanic eruption is stronger in low-end RCP scenarios, which is  
915 attributed to a warmer stratosphere and lower methane emissions. As methane reacts with chlorine in the atmosphere, higher  
916 methane emissions in the future will lead to lower stratospheric reactive chlorine species and thus suppress the ClO<sub>x</sub>-catalysed  
917 ozone loss. For the same model simulation under a low-end SSP scenario, we expect a stronger volcanic-induced ozone  
918 response and potentially a later year of shift in ozone response (net loss versus net gain, see Section 3.3). Future studies can  
919 design specific model experiments with the co-injection of halogen species and water vapour to quantify the timing of the shift  
920 in Antarctic ozone chemistry under different future emission scenarios.

Deleted: 1

Deleted: 8

Deleted: 9

Deleted: -9 DU,

Deleted: -

Deleted: +

Deleted: -2 DU,

Deleted: -

Deleted: +

Deleted: 0

Deleted: 2

Deleted: 0)

Deleted: in

Deleted: stratosphere (10-30 hPa)

Deleted: However

Deleted: ¶

O...

Deleted: are potentially important to

Deleted:

Deleted: Therefore, our estimated impacts represent a lower bound of the potential effects of future volcanic eruptions on ozone depletion. ...

Deleted: Recent chemistry-climate model simulations demonstrate that the co-injection of volcanic sulfur and halogens into the stratosphere can lead to greater ozone depletion compared to sulfur injections only (Staunton-Sykes et al., 2021). However, t

Deleted: and

Deleted: In addition to volcanic halogens, the emission of VSL chlorine and bromine compounds are crucial to project future ozone changes (Klobas et al., 2017; Bednarz et al., 2022).

Deleted:

Deleted: ¶

... [23]

959  
960  
961  
962  
963  
964  
965  
966  
967  
968  
969  
970  
971  
972  
973  
974  
975  
976  
977  
978  
979

#### 4 Conclusion

Using the plume-aerosol-chemistry-climate model UKESM-VPLUME with a stochastic representation of volcanic sulfur emissions, we quantified the effects of six stochastic scenarios on projected ozone recovery over Antarctica and Southern Hemisphere mid-latitudes. We showed that a high-end future eruption scenario delays the recovery of the Antarctic total column ozone and ozone mass deficit for up to 5 and 6 years respectively. These delays represented relatively small perturbations to the overall Antarctic and SH mid-latitudes ozone recovery. Our results also showed that the peak ozone loss due to large-magnitude volcanic eruptions in our stochastic scenarios weakens from 2015 to 2070 (Fig. 7c) as a result of declining CFC concentrations. Although our stochastic future eruption scenarios caused only a few years of delay in the ozone recovery metrics, large-magnitude eruptions can still potentially lead to substantial perturbations in stratospheric ozone prior to its recovery. For example, the mid-century eruption in the VOLC98 scenario led to an Antarctic ozone hole up to 5 million km<sup>2</sup> (Fig. 5c and 6d). Our results also showed that small-magnitude eruptions have little effect on the recovery of Antarctic and SH mid-latitudes stratospheric ozone. These results highlighted the importance of accounting for volcanic variability in assessing stratospheric ozone recovery over Antarctica and SH mid-latitudes. Volcanic eruptions along with other events that perturb the stratospheric aerosol layer, such as wildfires and deliberate stratospheric aerosol injections, remain as future challenges in assessing ozone recovery (WMO, 2022; Solomon et al., 2023; Chipperfield et al., 2024). Enhancing our understanding of volcano-induced ozone responses, including the effects of volcanic halogen emissions, is a crucial aspect for accurately assessing the healing of the Antarctic ozone layer. Continued improvements in models, volcanic emission datasets, and observational monitoring of the stratosphere will be critical to assess the stability and resilience of ozone layer recovery in the coming decades.

980  
981  
982  
983  
984  
985  
986  
987  
988  
989  
990  
991  
992  
993  
994  
995  
996  
997  
998  
999  
1000

#### Code availability

The code to reproduce the figures in the main text and supplementary information are available on Github:  
[https://github.com/maychim/volc\\_ozone](https://github.com/maychim/volc_ozone)

#### Data availability

The data used in this study are available here: 10.5281/zenodo.15838168

#### Author Contribution

MMC, TJA, and AS conceptualised the paper. MMC performed the UKESM simulations with the support from NLA. MMC performed the data analysis, visualisation, and wrote the first draft of the paper. HG, BJ, and SS provided critical feedback and helped shape the research and analysis. All authors discussed the results and commented on the manuscript.

#### Competing interest

The authors declare no competing interests.

#### Acknowledgements

We would like to thank Lauren Marshall, Alex Archibald and Maria Russo for their suggestions in the analysis. Special thanks to Martyn Chipperfield for his insightful feedback during the PhD viva, which contributed significantly to the improvement of this work. We would like to also thank James Keeble for providing the CMIP6 multi-model mean stratospheric ozone data, and Sandip Dhomse for providing the ML-TOMCAT ozone datasets. We would like to thank Bodeker Scientific for providing the BS-filled total column ozone database. This work used Monsoon2, a collaborative high-performance-computing facility

Deleted: sporadic  
Deleted: from future volcanic eruptions  
Deleted: y  
Deleted: X  
Deleted: future volcanic eruption  
Deleted:  
Deleted: over the 21st  
Deleted: century  
Deleted: chlorofluorocarbon  
Deleted: 8  
Deleted: 9

1012 funded by the Met Office and the Natural Environment Research Council, and JASMIN, the UK collaborative data analysis  
1013 facility.

1014

#### 1015 **Financial support**

1016 MMC is supported by the Croucher Foundation through the Croucher Fellowship. BJ was supported by the Met Office Hadley  
1017 Centre Climate Programme sponsored by the United Kingdom Department of Science, Innovation, and Technology (DSIT).  
1018 SS gratefully acknowledges support from NSF atmospheric chemistry grants 2128617 and 2316980.

#### 1019 **References**

1020 Aubry, T. J., Jellinek, A. M., Degruyter, W., Bonadonna, C., Radić, V., Clyne, M., and Quainoo, A.: Impact of global warming  
1021 on the rise of volcanic plumes and implications for future volcanic aerosol forcing, *JGR Atmospheres*, 121,  
1022 <https://doi.org/10.1002/2016JD025405>, 2016.

1023 Bethke, I., Outten, S., Otterå, O. H., Hawkins, E., Wagner, S., Sigl, M., and Thorne, P.: Potential volcanic impacts on future  
1024 climate variability, *Nature Clim Change*, 7, 799–805, <https://doi.org/10.1038/nclimate3394>, 2017.

1025 Bobrowski, N., Hönninger, G., Galle, B., and Platt, U.: Detection of bromine monoxide in a volcanic plume, *Nature*, 423, 273–  
1026 276, <https://doi.org/10.1038/nature01625>, 2003.

1027 Bodeker, G.E. and Kremser, S., Indicators of Antarctic ozone depletion: 1979 to 2019, *Atmos. Chem. Phys.*, doi:10.5194/acp-  
1028 21-5289-2021, 2021.

1029 [Brenna, H., Kutterolf, S., Mills, M. J., and Krüger, K.: The potential impacts of a sulfur- and halogen-rich supereruption such  
1030 as Los Chocoyos on the atmosphere and climate, \*Atmos. Chem. Phys.\*, 20, 6521–6539, \[https://doi.org/10.5194/acp-20-6521-  
2020\]\(https://doi.org/10.5194/acp-20-6521-<br/>1031 2020\), 2020.](#)

1032 Copernicus Atmosphere Monitoring Service (CAMS): Large and persistent 2023 ozone hole closes,  
1033 [https://atmosphere.copernicus.eu/large-and-persistent-2023-ozone-hole-  
closes#:~:text=The%202023%20ozone%20hole%20completed,longest%2Dlived%20observed%20to%20date](https://atmosphere.copernicus.eu/large-and-persistent-2023-ozone-hole-<br/>1034 closes#:~:text=The%202023%20ozone%20hole%20completed,longest%2Dlived%20observed%20to%20date), 2023.

1035 Carn, S.: Multi-Satellite Volcanic Sulfur Dioxide L4 Long-Term Global Database V4,  
1036 <https://doi.org/10.5067/MEASURES/SO2/DATA405>, 2021.

1037 Carn, S. A., Clarisse, L., and Prata, A. J.: Multi-decadal satellite measurements of global volcanic degassing, *Journal of  
1038 Volcanology and Geothermal Research*, 311, 99–134, <https://doi.org/10.1016/j.jvolgeores.2016.01.002>, 2016.

1039 Chim, M. M., Aubry, T. J., Abraham, N. L., Marshall, L., Mulcahy, J., Walton, J., and Schmidt, A.: Climate Projections Very  
1040 Likely Underestimate Future Volcanic Forcing and Its Climatic Effects, *Geophysical Research Letters*, 50, e2023GL103743,  
1041 <https://doi.org/10.1029/2023GL103743>, 2023.

1042 Chipperfield, M. P. and Bekki, S.: Opinion: Stratospheric ozone – depletion, recovery and new challenges, *Atmos. Chem.  
1043 Phys.*, 24, 2783–2802, <https://doi.org/10.5194/acp-24-2783-2024>, 2024.

Formatted: Font: 10 pt, Font colour: Custom Colour  
(RGB(33,33,33))

- 1044 [Dhomse, S. S., Emmerson, K. M., Mann, G. W., Bellouin, N., Carslaw, K. S., Chipperfield, M. P., Hommel, R., Abraham, N.](#)  
1045 [L., Telford, P., Braesicke, P., Dalvi, M., Johnson, C. E., O'Connor, F., Morgenstern, O., Pyle, J. A., Deshler, T., Zawodny, J.](#)  
1046 [M., and Thomason, L. W.: Aerosol microphysics simulations of the Mt. Pinatubo eruption with the UM-UKCA composition-](#)  
1047 [climate model, Atmos. Chem. Phys., 14, 11221–11246, <https://doi.org/10.5194/acp-14-11221-2014>, 2014.](#)
- 1048 Dhomse, S. S., Kinnison, D., Chipperfield, M. P., Salawitch, R. J., Cionni, I., Hegglin, M. I., Abraham, N. L., Akiyoshi, H.,  
1049 Archibald, A. T., Bednarz, E. M., Bekki, S., Braesicke, P., Butchart, N., Dameris, M., Deushi, M., Frith, S., Hardiman, S. C.,  
1050 Hassler, B., Horowitz, L. W., Hu, R.-M., Jöckel, P., Josse, B., Kimer, O., Kremser, S., Langematz, U., Lewis, J., Marchand,  
1051 M., Lin, M., Mancini, E., Maréchal, V., Michou, M., Morgenstern, O., O'Connor, F. M., Oman, L., Pitari, G., Plummer, D. A.,  
1052 Pyle, J. A., Revell, L. E., Rozanov, E., Schofield, R., Stenke, A., Stone, K., Sudo, K., Tilmes, S., Visioni, D., Yamashita, Y.,  
1053 and Zeng, G.: Estimates of ozone return dates from Chemistry-Climate Model Initiative simulations, Atmos. Chem. Phys., 18,  
1054 8409–8438, <https://doi.org/10.5194/acp-18-8409-2018>, 2018.
- 1055 Eric Klobas, J., Wilmouth, D. M., Weisenstein, D. K., Anderson, J. G., and Salawitch, R. J.: Ozone depletion following future  
1056 volcanic eruptions, Geophysical Research Letters, 44, 7490–7499, <https://doi.org/10.1002/2017GL073972>, 2017.
- 1057 Evan, S., Brioude, J., Rosenlof, K. H., Gao, R.-S., Portmann, R. W., Zhu, Y., Volkamer, R., Lee, C. F., Metzger, J.-M., Lamy,  
1058 K., Walter, P., Alvarez, S. L., Flynn, J. H., Asher, E., Todt, M., Davis, S. M., Thornberry, T., Vömel, H., Wienhold, F. G.,  
1059 Stauffer, R. M., Millán, L., Santee, M. L., Froidevaux, L., and Read, W. G.: Rapid ozone depletion after humidification of the  
1060 stratosphere by the Hunga Tonga Eruption, Science, 382, eadg2551, <https://doi.org/10.1126/science.adg2551>, 2023.
- 1061 Eyring, V., Arblaster, J. M., Cionni, I., Sedláček, J., Perlwitz, J., Young, P. J., Bekki, S., Bergmann, D., Cameron-Smith, P.,  
1062 Collins, W. J., Faluvegi, G., Gottschaldt, K. -D., Horowitz, L. W., Kinnison, D. E., Lamarque, J. -F., Marsh, D. R., Saint-  
1063 Martin, D., Shindell, D. T., Sudo, K., Szopa, S., and Watanabe, S.: Long-term ozone changes and associated climate impacts  
1064 in CMIP5 simulations, JGR Atmospheres, 118, 5029–5060, <https://doi.org/10.1002/jgrd.50316>, 2013.
- 1065 Fahey, D. W., Kawa, S. R., Woodbridge, E. L., Tin, P., Wilson, J. C., Jonsson, H. H., Dye, J. E., Baumgardner, D., Borrmann,  
1066 S., Toohy, D. W., Avallone, L. M., Proffitt, M. H., Margitan, J., Loewenstein, M., Podolske, J. R., Salawitch, R. J., Wofsy,  
1067 S. C., Ko, M. K. W., Anderson, D. E., Schoeber, M. R., and Chan, K. R.: In situ measurements constraining the role of sulphate  
1068 aerosols in mid-latitude ozone depletion, Nature, 363, 509–514, <https://doi.org/10.1038/363509a0>, 1993.
- 1069 [Fleming, E. L., Newman, P. A., Liang, Q., and Oman, L. D.: Stratospheric Temperature and Ozone Impacts of the Hunga](#)  
1070 [Tonga-Hunga Ha'apai Water Vapor Injection, JGR Atmospheres, 129, e2023JD039298,](#)  
1071 <https://doi.org/10.1029/2023JD039298>, 2024.
- 1072 Frith, S. M., Stolarski, R. S., Kramarova, N. A., and McPeters, R. D.: Estimating uncertainties in the SBUV Version 8.6 merged  
1073 profile ozone data set, Atmos. Chem. Phys., 17, 14695–14707, <https://doi.org/10.5194/acp-17-14695-2017>, 2017.
- 1074 [Hall, R. J., Mitchell, D. M., Seviour, W. J. M., and Wright, C. J.: Persistent Model Biases in the CMIP6 Representation of](#)  
1075 [Stratospheric Polar Vortex Variability, JGR Atmospheres, 126, e2021JD034759, <https://doi.org/10.1029/2021JD034759>,](#)  
1076 [2021.](#)
- 1077  
1078 Ivy, D. J., Solomon, S., Kinnison, D., Mills, M. J., Schmidt, A., and Neely, R. R.: The influence of the Calbuco eruption on  
1079 the 2015 Antarctic ozone hole in a fully coupled chemistry-climate model, Geophysical Research Letters, 44, 2556–2561,  
1080 <https://doi.org/10.1002/2016GL071925>, 2017.

Formatted

Formatted

1081 Keeble, J., Hassler, B., Banerjee, A., Checa-Garcia, R., Chiodo, G., Davis, S., Eyring, V., Griffiths, P. T., Morgenstern, O.,  
 1082 Nowack, P., Zeng, G., Zhang, J., Bodeker, G., Burrows, S., Cameron-Smith, P., Cugnet, D., Danek, C., Deushi, M., Horowitz,  
 1083 L. W., Kubin, A., Li, L., Lohmann, G., Michou, M., Mills, M. J., Nabat, P., Olivie, D., Park, S., Seland, Ø., Stoll, J., Wieners,  
 1084 K.-H., and Wu, T.: Evaluating stratospheric ozone and water vapour changes in CMIP6 models from 1850 to 2100, *Atmos.*  
 1085 *Chem. Phys.*, 21, 5015–5061, <https://doi.org/10.5194/acp-21-5015-2021>, 2021.

1086 [Klobas, E. J., Wilmouth, D. M., Weisenstein, D. K., Anderson, J. G., and Salawitch, R. J.: Ozone depletion following future  
 1087 volcanic eruptions, \*Geophysical Research Letters\*, 44, 7490–7499, <https://doi.org/10.1002/2017GL073972>, 2017.](#)

1088

1089 [Kovilakam, M., Thomason, L. W., Ernest, N., Rieger, L., Bourassa, A., & Millán, L. \(2020\). The Global Space-based  
 1090 Stratospheric Aerosol Climatology \(version 2.0\): 1979–2018. \*Earth System Science Data\*, 12\(4\), 2607–2634.  
 1091 <https://doi.org/10.5194/essd-12-2607-2020>](#)

1092 Lee, A. M., Jones, R. L., Kilbane-Dawe, I., and Pyle, J. A.: Diagnosing ozone loss in the extratropical lower stratosphere, *J.*  
 1093 *Geophys. Res.*, 107, <https://doi.org/10.1029/2001JD000538>, 2002.

1094 Mastin, L. G.: A user-friendly one-dimensional model for wet volcanic plumes, *Geochem Geophys Geosyst*, 8,  
 1095 2006GC001455, <https://doi.org/10.1029/2006GC001455>, 2007.

1096 Mastin, L. G.: Testing the accuracy of a 1-D volcanic plume model in estimating mass eruption rate, *JGR Atmospheres*, 119,  
 1097 2474–2495, <https://doi.org/10.1002/2013JD020604>, 2014.

1098 McElroy, M. B., Salawitch, R. J., Wofsy, S. C., and Logan, J. A.: Reductions of Antarctic ozone due to synergistic interactions  
 1099 of chlorine and bromine, *Nature*, 321, 759–762, 1986.

1100 Meinshausen, M., Nicholls, Z. R. J., Lewis, J., Gidden, M. J., Vogel, E., Freund, M., Beyerle, U., Gessner, C., Nauels, A.,  
 1101 Bauer, N., Canadell, J. G., Daniel, J. S., John, A., Krummel, P. B., Luderer, G., Meinshausen, N., Montzka, S. A., Rayner, P.  
 1102 J., Reimann, S., Smith, S. J., Van Den Berg, M., Velders, G. J. M., Vollmer, M. K., and Wang, R. H. J.: The shared socio-  
 1103 economic pathway (SSP) greenhouse gas concentrations and their extensions to 2500, *Geosci. Model Dev.*, 13, 3571–3605,  
 1104 <https://doi.org/10.5194/gmd-13-3571-2020>, 2020.

1105 [Mills, M. J., Schmidt, A., Easter, R., Solomon, S., Kinnison, D. E., Ghan, S. J., Neely, R. R., Marsh, D. R., Conley, A.,  
 1106 Bardeen, C. G., and Gettelman, A.: Global volcanic aerosol properties derived from emissions, 1990–2014, using CESM1  
 1107 \(WACCM\), \*J. Geophys. Res.-Atmos.\*, 121, 2332–2348, <https://doi.org/10.1002/2015JD024290>, 2016.](#)

1108 [Ming, A., Winton, V. H. L., Keeble, J., Abraham, N. L., Dalvi, M. C., Griffiths, P., Caillon, N., Jones, A. E., Mulvaney, R.,  
 1109 Savarino, J., Frey, M. M., and Yang, X.: Stratospheric Ozone Changes From Explosive Tropical Volcanoes: Modeling and Ice  
 1110 Core Constraints, \*JGR Atmospheres\*, 125, e2019JD032290, <https://doi.org/10.1029/2019JD032290>, 2020.](#)

1111 Molina, L. T. and Molina, M. J.: Production of chlorine oxide (ClO<sub>2</sub>) from the self-reaction of the chlorine oxide (ClO)  
 1112 radical, *Journal of Physical Chemistry*, 91, 433–436, 1987.

1113 Mulcahy, J. P., Jones, C. G., Rumbold, S. T., Kuhlbrodt, T., Dittus, A. J., Blockley, E. W., Yool, A., Walton, J., Hardacre,  
 1114 C., Andrews, T., Bodas-Salcedo, A., Stringer, M., De Mora, L., Harris, P., Hill, R., Kelley, D., Robertson, E., and Tang, Y.:

**Formatted:** Space After: 0 pt, Line spacing: 1.5 lines,  
 Border: Top: (No border), Bottom: (No border), Left: (No  
 border), Right: (No border), Between : (No border)

**Formatted:** German

**Deleted:** Millán, L., Santee, M. L., Lambert, A., Livesey, N. J.,  
 Werner, F., Schwartz, M. J., Pumphrey, H. C., Manney, G. L., Wang,  
 Y., Su, H., Wu, L., Read, W. G., and Froidevaux, L.: The Hunga  
 Tonga-Hunga Ha'apai Hydration of the Stratosphere, *Geophysical  
 Research Letters*, 49, e2022GL099381,  
<https://doi.org/10.1029/2022GL099381>, 2022.¶

- 1121 UKESM1.1: development and evaluation of an updated configuration of the UK Earth System Model, *Geosci. Model Dev.*,  
 1122 16, 1569–1600, <https://doi.org/10.5194/gmd-16-1569-2023>, 2023.
- 1123 NASA Ozone Watch, <https://ozonewatch.gsfc.nasa.gov/meteorology/SH.html>, 2024.
- 1124 O'Neill, B. C., Tebaldi, C., Van Vuuren, D. P., Eyring, V., Friedlingstein, P., Hurtt, G., Knutti, R., Kriegler, E., Lamarque, J.-  
 1125 F., Lowe, J., Meehl, G. A., Moss, R., Riahi, K., and Sanderson, B. M.: The Scenario Model Intercomparison Project  
 1126 (ScenarioMIP) for CMIP6, *Geosci. Model Dev.*, 9, 3461–3482, <https://doi.org/10.5194/gmd-9-3461-2016>, 2016.
- 1127 Prata, A. J., Carn, S. A., Stohl, A., and Kerkmann, J.: Long range transport and fate of a stratospheric volcanic cloud from  
 1128 Soufrière Hills volcano, Montserrat, *Atmos. Chem. Phys.*, 7, 5093–5103, <https://doi.org/10.5194/acp-7-5093-2007>, 2007.
- 1129 Pyle, D. M. and Mather, T. A.: Halogens in igneous processes and their fluxes to the atmosphere and oceans from volcanic  
 1130 activity: A review, *Chemical Geology*, 263, 110–121, <https://doi.org/10.1016/j.chemgeo.2008.11.013>, 2009.
- 1131 ~~Santee, M. L., Manney, G. L., Lambert, A., Millán, L. F., Livesey, N. J., Pitts, M. C., Froidevaux, L., Read, W. G., and Fuller,  
 1132 R. A.: The Influence of Stratospheric Hydration From the Hunga Eruption on Chemical Processing in the 2023 Antarctic  
 1133 Vortex, *JGR Atmospheres*, 129, e2023JD040687, <https://doi.org/10.1029/2023JD040687>, 2024.~~
- 1134 Sellar, A. A., Jones, C. G., Mulcahy, J. P., Tang, Y., Yool, A., Wiltshire, A., O'Connor, F. M., Stringer, M., Hill, R., Palmieri,  
 1135 J., Woodward, S., De Mora, L., Kuhlbrodt, T., Rumbold, S. T., Kelley, D. I., Ellis, R., Johnson, C. E., Walton, J., Abraham,  
 1136 N. L., Andrews, M. B., Andrews, T., Archibald, A. T., Berthou, S., Burke, E., Blockley, E., Carslaw, K., Dalvi, M., Edwards,  
 1137 J., Folberth, G. A., Gedney, N., Griffiths, P. T., Harper, A. B., Hendry, M. A., Hewitt, A. J., Johnson, B., Jones, A., Jones, C.  
 1138 D., Keeble, J., Liddicoat, S., Morgenstern, O., Parker, R. J., Predoi, V., Robertson, E., Siahhan, A., Smith, R. S., Swaminathan,  
 1139 R., Woodhouse, M. T., Zeng, G., and Zerroukat, M.: UKESM1: Description and Evaluation of the U.K. Earth System Model,  
 1140 *J Adv Model Earth Syst*, 11, 4513–4558, <https://doi.org/10.1029/2019MS001739>, 2019.
- 1141 Sigl, M., Toohey, M., McConnell, J. R., Cole-Dai, J., and Severi, M.: Volcanic stratospheric sulfur injections and aerosol  
 1142 optical depth during the Holocene (past 11 500 years) from a bipolar ice-core array, *Earth Syst. Sci. Data*, 14, 3167–3196,  
 1143 <https://doi.org/10.5194/essd-14-3167-2022>, 2022.
- 1144 Solomon, S., Ivy, D. J., Kinnison, D., Mills, M. J., Neely, R. R., and Schmidt, A.: Emergence of healing in the Antarctic ozone  
 1145 layer, *Science*, 353, 269–274, <https://doi.org/10.1126/science.aac0061>, 2016.
- 1146 Solomon, S., Dube, K., Stone, K., Yu, P., Kinnison, D., Toon, O. B., Strahan, S. E., Rosenlof, K. H., Portmann, R., Davis, S.,  
 1147 Randel, W., Bernath, P., Boone, C., Bardeen, C. G., Bourassa, A., Zawada, D., and Degenstein, D.: On the stratospheric  
 1148 chemistry of midlatitude wildfire smoke, *Proc. Natl. Acad. Sci. U.S.A.*, 119, e2117325119,  
 1149 <https://doi.org/10.1073/pnas.2117325119>, 2022.
- 1150 Stone, K. A., Solomon, S., Kinnison, D. E., and Mills, M. J.: On Recent Large Antarctic Ozone Holes and Ozone Recovery  
 1151 Metrics, *Geophysical Research Letters*, 48, e2021GL095232, <https://doi.org/10.1029/2021GL095232>, 2021.
- 1152 WMO: Scientific assessment of ozone depletion: Global Ozone Research and Monitoring Project – GAW Report no. 278,  
 1153 Geneva, Switzerland: World Meteorological Organization, ISBN: 978-9914-733-97-6, 2022.
- 1154

**Deleted:** Santee, M. L., Lambert, A., Froidevaux, L., Manney, G. L., Schwartz, M. J., Millán, L. F., Livesey, N. J., Read, W. G., Werner, F., and Fuller, R. A.: Strong Evidence of Heterogeneous Processing on Stratospheric Sulfate Aerosol in the Extratropical Southern Hemisphere Following the 2022 Hunga Tonga-Hunga Ha'apai Eruption, *JGR Atmospheres*, 128, e2023JD039169, <https://doi.org/10.1029/2023JD039169>, 2023.\*

1162 Yu, P., Davis, S. M., Toon, O. B., Portmann, R. W., Bardeen, C. G., Barnes, J. E., Telg, H., Maloney, C., and Rosenlof, K. H.:  
1163 Persistent Stratospheric Warming Due to 2019–2020 Australian Wildfire Smoke, *Geophysical Research Letters*, 48,  
1164 e2021GL092609, <https://doi.org/10.1029/2021GL092609>, 2021.

1165 Yung, Y., Pinto, J., Watson, R., and Sander, S.: Atmospheric bromine and ozone perturbations in the lower stratosphere,  
1166 *Journal of Atmospheric Sciences*, 37, 339–353, 1980.

1167 [Zhou, X., Dhomse, S. S., Feng, W., Mann, G., Heddell, S., Pumphrey, H., Kerridge, B. J., Latter, B., Siddans, R., Ventress,  
1168 L., Querel, R., Smale, P., Asher, E., Hall, E. G., Bekki, S., and Chipperfield, M. P.: Antarctic Vortex Dehydration in 2023 as  
1169 a Substantial Removal Pathway for Hunga Tonga-Hunga Ha’apai Water Vapor, \*Geophysical Research Letters\*, 51,  
1170 e2023GL107630, <https://doi.org/10.1029/2023GL107630>, 2024.](#)

1171 Zhu, Y., Toon, O. B., Kinnison, D., Harvey, V. L., Mills, M. J., Bardeen, C. G., Pitts, M., Bègue, N., Renard, J., Berthet, G.,  
1172 and Jégou, F.: Stratospheric Aerosols, Polar Stratospheric Clouds, and Polar Ozone Depletion After the Mount Calbuco  
1173 Eruption in 2015, *JGR Atmospheres*, 123, <https://doi.org/10.1029/2018JD028974>, 2018.

1174 [Zhu, Y., Bardeen, C. G., Tilmes, S., Mills, M. J., Wang, X., Harvey, V. L., Taha, G., Kinnison, D., Portmann, R. W., Yu, P.,  
1175 and others: Perturbations in stratospheric aerosol evolution due to the water-rich plume of the 2022 Hunga-Tonga eruption,  
1176 \*Communications Earth & Environment\*, 3, 248, 2022.](#)

1177 [Zhuo, Z., Wang, X., Zhu, Y., Yu, W., Bednarz, E. M., Fleming, E., Colarco, P. R., Watanabe, S., Plummer, D., Stenchikov,  
1178 G., Randel, W., Bourassa, A., Aquila, V., Sekiya, T., Schoeberl, M. R., Tilmes, S., Zhang, J., Kushner, P. J., and Pausata, F.  
1179 S. R.: Comparing multi-model ensemble simulations with observations and decadal projections of upper atmospheric variations  
1180 following the Hunga eruption, \*Atmos. Chem. Phys.\*, 25, 13161–13176, <https://doi.org/10.5194/acp-25-13161-2025>, 2025.](#)

1183 ▲

Formatted

Formatted: Font: 10 pt, Not Bold,